Journal of Materials Chemistry A

Accepted Manuscript

ROYAL SOCIETY OF CHEMISTRY

www.rsc.org/materialsA

Journal of Materials Chemistry A

Dynamic Article Links ►

Cite this: DOI: 10.1039/c0xx00000x

www.rsc.org/xxxxxx

ARTICLE TYPE

Purification of Phenol-contaminated Water by Adsorption with Quaternized poly(dimethylaminopropyl methacrylamide)-grafted PVBC Microspheres

Juntao Gu,[a] Shaojun Yuan,[a,*] Yu Zheng,[a] Wei Jiang,[a] Bin Liang,[a] Simo O Pehkonen,[b]

Received (in XXX, XXX) Xth XXXXXXXXX 2014, Accepted Xth XXXXXXXXX 20XX

DOI: 10.1039/b000000x

Cross-linked poly(vinylbenzyl chloride) (PVBC) microspheres tethered with polymer brushes containing quaternary ammonium ions were developed as an anionic adsorbent for the efficient removal of phenol from aqueous solutions. The terminal alkyl chlorine groups on the PVBC microspheres were served as anchor sites for the grafting of poly(*dimethylaminopropyl methacrylamide*) (PDMAPMA) brushes via surface-initiated atom transfer radical polymerization (ATRP). The pendent tertiary amino groups of the PDMAPMA chains were converted into quaternary ammonium ions by *N*-alkylation reaction to produce anionic adsorption functionality. Success in each reaction step was ascertained by Fourier transform infrared (FTIR), X-ray photoelectron spectroscopy (XPS) and scanning electron microscopy (SEM). Batch adsorption results demonstrated that solution pH values in a wide range of 3.0 - 11.0 had no evident effect on phenol adsorption by the quaternized PDMAPMA-grafted PVBC (i.e. PVBC-*g*-QPDMAPMA) microspheres, and that the adsorption capacity of the microspheres increased evidently with the grafting density of the quaternized PDMAPMA brushes within 6 h. The so-synthesized anionic adsorbents had a rapid pseudo-first-order-adsorption kinetic (equilibrium achieved within 60 min), and the Langmuir model-fitted maximum adsorption capacity of phenol was around 2.23 mmol·g^{-1} at pH 6.5 with an initial concentration of 1.05 – 5.31 mmol·L^{-1} (i.e. 100 - 500 mg·L^{-1}). The calculated thermodynamic parameters revealed an exothermic and spontaneous adsorption process of phenol onto the quaternized QPDMAPMA-grafted microspheres. Desorption and adsorption cycle experiments demonstrated that the anionic adsorbents loaded with phenol were found to be readily regenerated in a 0.1 mol·L^{-1} NaOH solution, and that the adsorption capacity decreased by less than 10% upon five cycles.

1. Introduction

The hazardous organic compounds-polluted ground water and surface water have attached worldwide attention over decades. Phenol and its derivatives are one of the largest groups of environmentally organic pollutants due to their presence in the wastewater from many industrial processes, such as the production of oil and oil products, furnace coke, steel, explosives, paint, cork and fiberglass, the production and recycling of rubber goods, the textile industry, some branches of the food and beverage industry, and the pharmaceutical industry.[1] Their presence in aqueous solution even at low concentrations can pose a severe risk to living organisms, for example, phenol concentration at more than 10 mg·L^{-1} can cause death of most aquatic life within 96 h.[2] The harmful effects of phenol have been widely recognized on the brain, digestive system, eyes, heart, kidney, liver, lungs, and skin.[3] Because of their toxicity and carcinogenicity, phenolic compounds have been included in the US Environmental Protection Agency (EPA) list of priority pollutants, with a maximum concentration level of 1 mg·L^{-1} for public sewers. Therefore, it is of great significance to remove the phenol pollutants from waste streams before discharging them into the sewer systems or the receiving bodies of water.

Different strategies have been developed to address the growing need for the removal or destruction of phenolic compounds from aqueous solutions, such as biological treatment using anaerobic granular sludge,[4] catalytic wet oxidation,[5] photo-catalytic treatment,[6] solvent extraction,[7] reverse osmosis[8] and adsorption.[9] Among them, adsorption is by far the most efficient, economic and versatile method, especially if combined with appropriate regeneration steps, since the adsorption process can completely eradicate the pollutants from the wastewater without leaving behind any toxic by-product. Various materials have been used as adsorbents for the removal of phenol from aqueous solutions, including activated carbon,[10, 11] biosorbents (such as chitosan[12] and dried activated sludge[13]), polymeric adsorbents,[14] fly ash,[15] zeolite,[16] soil,[17] coal,[18] red mud,[19] and sewage sludge.[20] Although activated carbons, the most commonly used adsorbent for the phenol removal, exhibit satisfactory performance for the removal

[a] *Multiphase Mass Transfer & Reaction Engineering Lab, College of Chemical Engineering, Sichuan University, Chengdu, China 610065. Fax: 86 28 85460556; Tel: 86 28 85990133;*

Email: yuanshaojun@gmail.com

[b] *Department of Environmental Sciences, University of Eastern Finland, 70211 Kuopio, Finland*

Electronic Supplementary Information (ESI) available: [details of any supplementary information available should be included here]. See DOI: 10.1039/b000000x/

of phenol from wastewater, the main concerns of these adsorbents are the high regeneration cost, the generation of carbon fines and the poor selectivity to recover specific organic chemicals.[21] Thus, an alternative adsorbent with highly regenerable and stable properties is highly desired for the phenol removal from the aqueous solution.

Polymeric adsorbents are considered as a potential alternative adsorbent to remove the organic contaminants such as phenol and its derivatives from wastewater due to their chemically-inert feature, low cost, ease of regeneration, high adsorption capacity and limited toxicity,[22] Particularly, the regeneration of polymeric sorbents can be accomplished by a simple and nondestructive solvent washing process. This provides an opportunity to recover the solute from the wastewater system. The polymeric adsorbent materials are generally divided into two categories, i.e. the natural polymers, such as chitin,[23] poly(humic acid),[24] chitosan[12] and biomass (alga),[25] and the synthetic polymers, such as poly(hydroxyethyl methacrylate) (PHEMA),[26] poly(methyl methacrylate) (PMAA),[27] poly(glycidyl methacrylate) (PGMA),[28] poly(styrene) (PS),[29] and so on. The hypercrosslinked synthetic polymeric resins have been found to be effective adsorbents for the removal of phenolic compounds. Over the past decades, the synthetic polymeric adsorbents have attracted considerable attention for removing organic pollutants from industrial and municipal wastewater.

The poly(vinylbenzyl chloride) (PVBC), as a typical PS-type synthetic polymers, has been employed in synthesizing high-efficient adsorbents for the removal of metal ions or organic pollutants from wastewater in recent years,[30, 31] because the abundant chloromethyl groups of the PVBC surface can serve as anchor sites to introduce specific functional groups, such as amino groups (-NH_2), hydroxyl groups (-OH), carboxylate (-COOH) and sulfonic groups (-SO_3H), for the enhanced adsorption capacity and selectivity of polymeric adsorbents.[32] Different approaches have been reported to prepare PVBC-based adsorbents, including amination of PVBC and subsequent alkaline ion exchange to produce polyvinyl benzyl trimethylammonium hydroxide (PVBTAH)-zeolitic imidazolate framework (ZIF-8),[33] grafting of PVBC beads with primary amines,[34, 35] amino methane sulfonic acid,[36] proline,[37] and aminocarboxylic acid,[38] quaternization of the PVBC microspheres with ethyl piperazine,[39] and *N,N*-dimethylethanolamine (DMEA).[40] Among these methods, surface-initiated atom transfer radical polymerization (SI-ATRP) provides a versatile approach to precisely prepare functional polymer brushes of narrow polydispersity, well-defined architecture, controllable thickness, and composition.[41] The PVBC resins have been modified via SI-ATRP by grafting of different functional polymer brushes, including *N,N*-dimethylaminoethyl methacrylate (PDMAEMA), [42, 43] PMMA,[44] PGMA,[45] poly(vinyl-pyridine) (P4VP),[46] and poly(acrylonitrile)-*co*-poly(*tert*-butyl acrylate) (PAN-*co*-PtBA),[47] for the effective removal of heavy metal ions or organic pollutants from aqueous solution. However, to the best of our knowledge, only few studies have been documented to functionalize PVBC via SI-ATRP for the enhancement of phenol removal from aqueous solutions.[48]

Accordingly, the aim of this study is to tailor PVBC microspheres with quaternized poly*(*dimethylaminopropyl methacrylamide*)* (PDMAPMA) brushes as anionic adsorbents for the effective removal of phenol from aqueous solutions, and to explore the effect of different factors on the adsorption behavior. The microsphere substrate is chosen owing to its advantages of large specific surface area, high adsorption capacity, good diffusibility and mobility, uniform size distribution, easy recovery and handling from the dispersion. As shown schematically in Figure 1, the cross-linked PVBC microspheres were first synthesized using *in situ* suspension polymerization, followed by grafting of functional PDMAPMA brushes via surface-initiated ATRP. Finally, the pendent tertiary amino groups on the side chain of the PDMAPMA brushes were quaternized by alkyl bromides to produce the quaternary ammonium groups with cationic polyelectrolyte features, which can provide attractive electrostatic interactions for phenol adsorption. The quaternized PDMAPMA-grafted PVBC microspheres are expected not only to significantly increase the number of adsorption sites for the enhanced uptake capacity of phenol, but also to be readily regenerated for recycled use. Success in each functionalization step was ascertained by attenuated total reflectance-Fourier transform infrared (ATR-FTIR), *X*-ray photoelectron spectroscopy (XPS), and scanning electron microscopy (SEM). The effects of pH, salt effect and the grafting density of PDMAPMA brushes on the adsorption behavior of phenol were investigated. The adsorption kinetics, isotherms and thermodynamic parameters of the phenol on the quaternized PDMAPMA-grafted PVBC microspheres were also determined.

In a whole, the main novelties of this study are summarized as follows: (i) few studies have documented to graft quaternized PDMAPMA brushes (i.e. quaternary ammonium ions) onto the cross-linked PVBC resin surface via surface-initiated ATRP for phenol removal, although this approach has been utilized to graft various functional polymer brushes onto the resins for wastewater purification in recent years, (ii) most of phenol adsorbents were commonly applicable to acidic conditions, and took at least a few hours (or even days) to reach adsorption equilibrium. However, the synthesized cationic PDMAPMA-grafted resin possesses a desirable high adsorption capacity in a wide pH range of 3.0 – 11.0, and exhibits a rapid adsorption kinetic to attain the adsorption equilibrium in only 60 minutes, (iii) The postulated mechanism of the adsorbents containing quaternary ammonium ions is proposed to interpret the adsorption behaviors of phenol, which has been seldom reported previously.

2. Experimental

2.1 Materials

4-Vinylbenzyl chloride (VBC, 90%) was purchased from TCI Development Co. (Shanghai, China). *N*-[3-(dimethylamino)propyl] methacrylamide (DMAPMA, 98%), *N,N,N′,N″,N‴*-pentamethyldiethylenetriamine (PMDETA, 99%), copper (I) chloride (CuCl, 99%), and copper (II) chloride ($CuCl_2$, 97%) were obtained from Sigma–Aldrich Chemical Co (St. Louis, MO). Ethylene glycol dimethacrylate (EGDMA, 98%), potassium ferriccyanide ($K_3Fe(CN)_6$, 99.95%), poly(vinyl alcohol) (PVA, 87-89% hydrolyzed, average M.W. 88000), 4-amino-antipyrine, 2,2'-azobis(2-methylpropionitrile) (AIBN, 97%) were obtained from Best Reagent Co. (Chengdu, China). Bromoethane (CH_3CH_2Br, >98%) was purchased from Aladdin Reagent Co. (Shanghai, China). Other chemicals, such as phenol (>99%), NH_4Cl, NaCl, $NaNO_3$, and EDTA, and solvents, such as tetrahydrofuran (THF), ethanol, and toluene, were purchased from Changzheng Chemical Reagent Co. (Chengdu, China). All the other reagents were of analytical grade and used as received, unless otherwise stated. The deionized water used in the following experiments was purified using an Ulupure reverse osmosis system (Chengdu Ultrapure Technology Co., China).

2.2. Preparation of Cross-linked PVBC microspheres

The cross-linked PVBC microspheres were prepared by a suspension polymerization method described in detail previously.[42] Briefly, VBC (10.0 mL, 63.8 mmol), EGDMA (3 mL, 15.6mmol), and AIBN (0.24 g, 1.42 mmol) were dissolved in toluene (7.5 mL). The resulting solution was subsequently dispersed into 160 mL deionized water containing 0.5 g of PVA under continuous stirring in a 500 mL of round-bottom flask after the aqueous phase was purged with N_2 stream for about 30 min. The free radical polymerization reaction was allowed to proceed at 78 ^oC for 8 h at a stirring speed of 500 rpm. At the end of the polymerization reaction, the PVBC microspheres were harvested by filtration and were resuspended into a 500 mL of the ethanol/deionized water mixture (v:v, 1:1) for 12 h under continuous stirring. Finally, the PVBC microspheres were washed with copious amount of ethanol and deionized water prior to being dried at 50 ^oC in a vaccum oven. The microspheres were sieved to choose a size range of 600 – 900 μm in diameter for subsequent modification reaction and adsorption experiments.

2.3 Grafting of PDMAPMA brushes onto the PVBC microspheres and *N*-alkylation of PDMAPMA

The chloromethyl groups on the PVBC surface provide abundant initiators for the grafting of PDMAPMA brushes via surface-initiated ATRP of DMAPMA. Typically, 9 mL of DMAPMA (50 mmol) and 15mL of THF were introduced to a 50 ml round-bottom flask. The mixtures stirred and degassed with ultrapure nitrogen for 30 min, followed by feeding the PMDETA (ligand), CuCl (catalyst), $CuCl_2$ (deactivator) at a ratio of [DMAPMA]:[CuCl]:[$CuCl_2$]:[PMDETA] = 100:1.0:0.1:2.0. The reaction was allowed to proceed at 50 ^oC for a predetermined time. After the reaction, the resultant PDMAPMA-grafted microspheres (referred to as the PVBC-*g*-PDMAPMA) were thoroughly washed with copious amount of acetone and deionized water to remove the physically-adsorbed reactants, if any. The PVBC-*g*-PDMAPMA microspheres were subsequently dried under reduced pressure at 40 ^oC for 48 h prior to being stored in a vacuum desiccator. The PDMAPMA-grafted PVBC microspheres from 2 and 6 h of ATRP reaction were defined as PVBC-*g*-PDMAPMA1 and PVBC-*g*-PDMAPMA2 surfaces, respectively.

The PDMAPMA brushes were directly converted by *N*-alkylation reaction with bromoethane to the polycationic chains with quaternary ammonium groups using a similar procedure described previously.[49] Briefly, 0.5 g of PDMAPMA-grafted PVBC microspheres were immersed in a mixture of bromoethane (4 mL) and THF (2 mL) in a 25 ml round bottom flask. The mixture was magnetically stirred at 150 rpm and 45 ^oC to proceed the quaternization reaction for 24 h. After the reaction, the quaternized PVBC-*g*-PDMAPMA microspheres were washed thoroughly with copious amount of acetone and deionized water before being dried under reduced pressure at 40 ^oC until constant weight. The quaternized PVBC-*g*-PDMAPMA1 and PVBC-*g*-PDMAPMA2 surfaces were referred to as PVBC-*g*-QPDMAPMA1 and PVBC-*g*-QPDMAPMA2 surfaces, respectively.

2.4. Grafting density of PDMAPMA brushes on the PVBC microspheres

The polymerization time was used as an independent variable to control grafting yield (GY) of DMAPMA on the PVBC microsphere surface. GY was determined by measurement of the increase in the mass percentage of the PVBC-*g*-PDMAPMA microspheres. The grafting yield (GY) was defined by the following equation: [50]

$$GY(\%) = \frac{W_g - W_o}{W_o} \times 100\% \quad (1)$$

where W_g and W_o are the weights of the dry PVBC microspheres before and after the grafting of PDMAPMA brushes, respectively. The grafting density (GD) of PDMAPMA brushes on the PVBC microspheres as a function of polymerization time was calculated using the previously-reported equation:[51]

$$GD = \frac{(W_g - W_o)/M}{W_o} \quad (2)$$

where M is the molecular weight of DMAPMA repeat unit (i.e. 170.25 g/mol) of the PDMAPMA chains. The GY and GD values were the mean values from at least three replicate measurements.

2.5. Surface characterization

The PVBC microspheres before and after modification were characterized by SEM, ATR-FTIR and XPS. The change in surface morphology of the PVBC microspheres before and after graft polymerization, as well as the quaternization reaction, was observed at different magnifications (50× and 500×) using a JEOL SEM (JSM-7500F) under an accelerating voltage of 5 KV. All the samples were sputter-coated with a platinum ultrathin film prior to being mounted on a sample stub for SEM imaging. Chemical compositions of the PVBC, PVBC-*g*-PDMAPMA and PVBC-*g*-QPDMAPMA microsphere surfaces were determined by ATR-FTIR and XPS measurements. The ATR-FTIR measurements were performed on a Spectrum GX FTIR spectrometer (Perkin Elmer Inc., Waltham, MA) equipped with a smart ATR performer accessory using a germanium (Ge) crystal with an incident angle of 45° and a sampling area of 2 mm^2. The microspheres were mounted onto the Ge crystal, and the spectra were collected in a wavelength range of 4000-600 cm^{-1} at 4 cm^{-1} resolution over 64 scans. The XPS analyses of the pristine and modified PVBC microspheres, as well as the quaternized microspheres after phenol adsorption were conducted on a Kratos AXIS Hsi spectrometer under monochromatized Al KaX-ray radiation (1486.6 eV) using similar procedures described in detail previously.[52] The microspheres were sieved by Tyler Sieve to choose a size range of 600 – 900 μm in diameter, and the average diameters were subsequently determined in light of size distribution.

2.6 Adsorption features of quaternized PDMAPMA-grafted microspheres

The adsorption behavior of phenol on the PVBC-g-QPDMAPMA microspheres, including pH effect, sorption kinetics, isotherms, thermodynamic parameters, ionic strength effect, was determined by batch sorption experiments. All batch adsorption experiments were conducted at 25°C and 150 rpm in a thermostatically orbital shaker for 24 h with 0.1 g of microsphere adsorbents in 250 mL flasks containing 100 mL of phenol solution. The microspheres were removed by filtration, and the filtrates were collected to measure the final phenol concentration. The initial concentration of phenol for batch adsorption experiments was chosen to be 200 ppm (i.e. 2.13 $mmol \cdot L^{-1}$), since the phenol concentration in industrial wastewater such as petrochemical industry, benzene refinery, ammonia factory, and glass fiber factories is typically in a range of 200 – 500 ppm.[18] The concentrations of phenol were determined by the well-known 4-aminoantipyrine spectrophotometric method using procedures as those described previously,[53] on a TU-1810 UV-Vis spectrophotometer (PERSEE, Beijing, China) at 504 nm. The blank solution that does not contain phenol was used as control to calibrate the phenol measurement. All the experiments were conducted in duplicate, and the mean values were adopted. The calibration curves of the aqueous phenol solution at a concentration of 0.48, 1.44, 2.40, 3.84, and 4.80 $mg \cdot L^{-1}$ and the corresponding UV-spectra were illustrated in Supporting Information (Fig. S1). For comparison purposes, the sorption behavior was also studied for the pristine PVBC microspheres under the same experimental condition.

2.6.1 Effect of grafting yield

To determine the effect of graft yield on the sorption of phenol on the quaternized PDMAPMA-grafted microspheres, the quaternized microspheres with different grafting yield of DMAPMA (0 – 15.1%) were directly added into the 250 flaks containing 100 mL of phenol solution with an initial concentration of 200 $mg \cdot L^{-1}$ (i.e. 2.13 $mmol \cdot L^{-1}$). The flasks were shaken in a thermostatically orbital shaker under 150 rpm at 25°C for 24 h. The equilibrium adsorption capacity was calculated by the following equation:[43]

$$q_e = \frac{(C_o - C_e)v}{m} \quad (3)$$

where q_e is the equilibrium adsorption capacity ($mg \cdot g^{-1}$), C_o and C_e are the concentrations of the initial phenol solution and the final solution at equilibrium, respectively, m is the mass of grafted microspheres (g), and v is the volume of the solution (L), which remained constant throughout the adsorption period.

2.6.2 Effect of pH values

The optimal pH values for the quaternized microspheres were determined by investigating the adsorption profiles of phenol at various initial pH values of 3.0- 11.0. A 0.1 g of the quaternized PDMAPMA-grafted microspheres from 6 h of ATRP reaction was added, into a 200 $mg \cdot L^{-1}$ (i.e. 2.13 $mmol \cdot L^{-1}$) phenol solution with a predescribed pH value. The pH values of phenol solution were kept constant throughout the adsorption experiment by adding 0.1 $mol \cdot L^{-1}$ HCl or NaOH solution for every 2 h. The adsorption of phenol on the quaternized microspheres was allowed to proceed at 25°C under 150 rpm for 24 h. The adsorption capacity of the microspheres at different pH values was also calculated using the above equation 3.

2.6.3 Adsorption kinetics

In the adsorption kinetics experiment, a 0.1 g aliquot of the quaternized PDMAPMA-grafted microspheres (i.e. PVBC-*g*-QPDMAPMA2) from 6 h of ATRP reaction were added in 100 mL of phenol solution with the initial concentration of 200 $mg \cdot L^{-1}$ (i.e. 2.13 $mmol \cdot L^{-1}$), and the initial pH value of 6.5. Solution pH values were not adjusted during the adsorption process since they kept relatively constant (<±0.2). Aliquots of 1.0 mL phenol solution were taken at different time intervals, and the concentration variations of phenol were analyzed. The adsorbed amounts of phenol per unit weight of the microspheres at time t, q_t ($mg \cdot g^{-1}$), were calculated from the following equation:[54]

$$q_t = \frac{(C_o - C_t)v}{m} \quad (4)$$

where C_o and C_t ($mg \cdot L^{-1}$) correspond to the initial concentration of phenol and the phenol concentration of phenol at time t, respectively. v is the volume of the residual volume at time t, and m is the weight of the microspheres added..

2.6.4 Adsorption isotherms

The adsorption capacity of the quaternized PDMAPMA-grafted microspheres from 6 h of ATRP reaction at given temperatures were measured to obtain adsorption isotherms. The phenol solution was adjusted to a pH value of 6.5 ± 0.1 throughout the sorption period to obtain a series of working solutions with different initial concentration of 100 - 500 mg·L^{-1} (i.e. 1.05 – 5.31 mmol·L^{-1}). An aquilot of 0.1 g microspheres were added into100 mL of phenol solution and were shaken at 150 rpm for 24 h at different temperatures of 25, 35, 45, and 55 ^{o}C, respectively. The adsorption capacity of phenol onto the microsphere at equilibrium was estimated from the aforementioned equation 3.

2.6.5 Salt Effect on the adsorption of phenol on the quaternized microspheres

To investigate the salt effect on the adsorption behavior of phenol, different concentrations of NaCl, $NaNO_3$, and EDTA were added into the phenol solution with the initial concentration of 200 mg·L^{-1} (i.e. 2.13 mmol·L^{-1}), respectively. The concentration of NaCl and $NaNO_3$ was controlled in a range of 0.05 - 0.2 mol·L^{-1}, while the concentration of EDTA was kept at 0.005 - 0.05 mol·L^{-1}. The solution pH values remained constant at 6.5 ± 0.1 throughout by adjusting 0.1 mol·L^{-1} HCl or NaOH solution for every 2 h. The adsorption of phenol onto the PVBC-*g*-QPDMAPMA2 microspheres (0.1 g) was allowed to proceed for 24 h at 25 ^{o}C and 150 rpm in the thermostatically orbital shaker.

2.6.6 Regeneration of the quaternized PDMAPMA-grafted microspheres

The phenol-loaded microspheres were regenerated with 0.1 mol·L^{-1} NaOH solution using a similar procedure described in detail previously.[55] Briefly, the sorption experiments were conducted with 0.1 g of the microspheres in 100 ml of 200 mg·L^{-1} (i.e. 2.13 mmol·L^{-1}) phenol solution (pH at 6.5) at 25 ^{o}C and 150 rpm for 24 h. Subsequently, the phenol-loaded microspheres were collected by filtration, and were immersed in 200 mL of a 0.1 mol·L^{-1} NaOH solution at 25 ^{o}C and 150 rpm for 2 h to desorb the phenol. Finally, the absorbents were collected, washed with copious amounts of deionized water, and reused in the next cycle of adsorption. The sorption-desorption experiment was conducted for five cycles.

3. Results and discussion

The preparation of the quaternized PDMAPMA-grafted PVBC microspheres was schematically illustrated in Figure 1. The process includes: (i) the synthesis of crosslinked PVBC microspheres via suspension polymerization of VBC and EGDMA, (ii) the preparation of PVBC-*g*-PDMAPMA microspheres via surface-initiated ATRP of DMAPMA, and (iii) *N*-alkylation of the PDMAPMA brushes with bromoethane to produce the polycationic chains containing quaternary ammonium groups. Details of each functionalization step are discussed below.

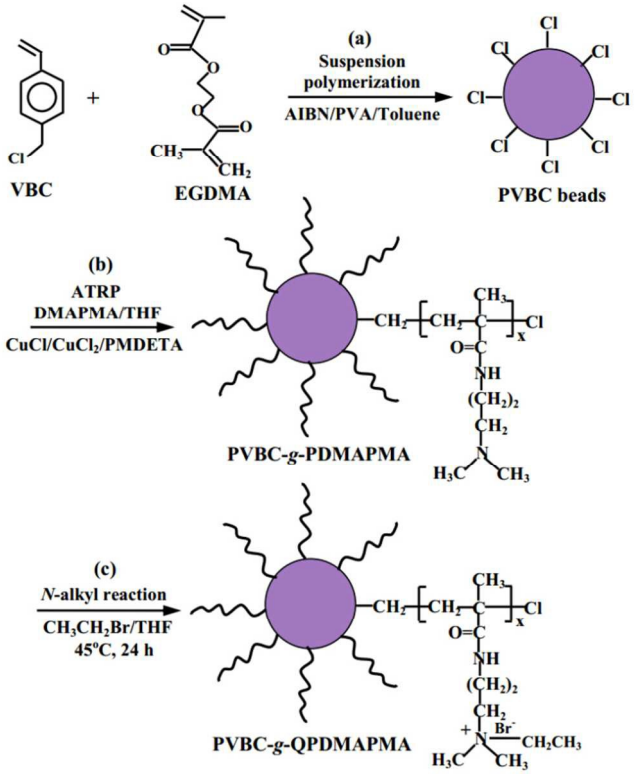

Figure 1 Schematic illustration of a three-step synthesis process of the cationic PVBC-*g*-QPDMAPMA microspheres: (a) the suspension polymerization of VBC and EGDMA to synthesize cross-linked PVBC microspheres, (b) surface-initiated ATRP of DMAPMA from the PVBC microsphere surfaces to graft the PDMAPMA brushes (i.e. the PVBC-*g*-PDMAPMA surfaces), and (c) subsequent quaternization of the PDMAPMA brushes to produce the quaternary ammonium groups (i.e. the PVBC-*g*-QPDMAPMA surfaces).

3.1 Surface Morphology

The surface morphologies and shape of the cross-linked PVBC microspheres before and after functionalization were characterized by SEM imaging. Figure S2 illustrates the optical micrographs and SEM images at different magnifications of the pristine and functionalized PVBC microspheres (Supporting Information). All the PVBC microspheres before and after surface functionalization are perfectly spherical in shape. The pristine cross-linked PVBC microsphere shows a white color and relatively smooth surface (Figs. S2a and S2b). The size of the pristine PVBC microspheres is fairly uniform with an average diameter of about 695 ± 4μm (Figs. S2b and S2c). Upon grating of PDMAPMA brushes for 6 h of ATRP reaction, the color of the microspheres changes to amber (Fig. s2d), but the surfaces of microspheres appear to remain relatively smooth without noticeable increase in surface roughness (Figs. S2e and 22f), indicating that the grafting of PDMAPMA brushes onto the microsphere surface is in a uniform manner. The size of the PDMAPMA-grafted PVBC microspheres has a noticeable increase after 6 h of ATRP reaction, as compared to that of

the PVBC microsphere, to around 706 ± 3 μm in averaged diameter (Fig. S2e). The subsequent quaternization of the PDMAPMA brushes can not only result in the change of microsphere color to dark violet (Fig. S2g), but also cause a slight increase in surface roughness (Fig. S2i). Therefore, the grafting of dense and thick quaternized PDMAPMA brushes onto the PVBC microspheres are expected to change the surface properties and substantially enhance its adsorption capacity toward phenol.

3.2 Preparation of PVBC microspheres and grafting of PDMAPMA brushes

In this study, the cross-linked PVBC microspheres were prepared by suspension polymerization with VBC as monomer, EGDMA as cross-linker, AIBN as initiator, and PVA as the stabilizing agent. Upon sieving, the particle size of the PVBC microspheres distributed in a range of 600 – 900 μm is used for the subsequent reaction. Earlier studies have demonstrated that methyl chloride is an effective initiator for surface-initiated ATRP from a variety of substrates. The cross-linked PVBC microsphere itself contains abundant chloromethyl groups as initiation sites to directly used for grafting of PDMAPMA brushes. Among all modification steps, the surface-initiated ATRP of DMAPMA monomer is the crucial step to prepare the quaternized PDMAPMA-grafted PVBC adsorbents with high adsorption capacities, which dominates the length of PDMAPMA brushes and the numbers of subsequent adsorption sites for adsorbates.

In surface-initiated ATRP reaction, the degree of grafting is mainly controlled by varying the monomer concentration and the reaction time.[41] The effect of ATRP reaction time on the grafting density was investigated to determine the kinetics of the PDMAPMA chain growth from the PVBC microsphere surfaces. Figure 2 shows the change in the grafting yield (GY) and grafting density (GD) of PDMAPMA brushes on the PVBC microsphere surfaces as a function of the reaction time. An approximate linear increase in the GY of the surface-grafted PDMAPMA brushes with reaction time can be observed for the PVBC-*g*-PDMAPMA surfaces, indicative of the living/controlled feature of the surface-initiated ATRP of DMAPMA. After 6 h of ATRP reaction, the GY value reaches as high as 15.07%. Similarly, the grafting density (GD) of the PDMAPMA brushes on the microsphere surface increases linearly with the ATRP reaction time, which further confirm a well-controlled manner of the growth of PDMAPMA chains. The GD value of the PDMAPMA brushes is estimated to be 0.89 mmol·g^{-1} after 6 h of the ATRP reaction. Thereby, the longer PDMAPMA brushes are able to form on the PVBC microsphere surfaces with increasing ATRP time to produce more reaction sites for quaternization. The resultant PDMAPMA-grafted surfaces from 2 and 6 h of ATRP time are defined as the PVBC-*g*-PDMAPMA1 and PVBC-*g*-PDMAPMA2 surfaces. The surface chemistry of the PVBC microspheres before and after graft polymerization was characterized by ATR-FTIR and XPS to ascertain the synthetic reactions.

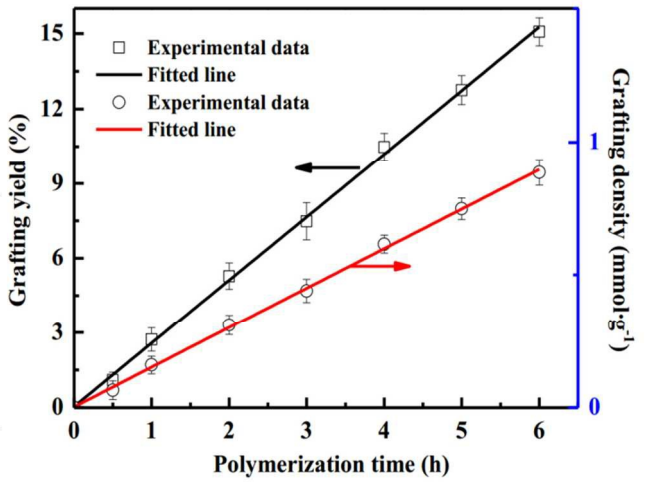

Figure 2 A linear relationship of the graft yield (GY) and grafting density (GD) of the PDMAPMA brushes formed on the surfaces of the PVBC-*g*-PDMAPMA microspheres as a function of ATRP time.

3.2.1 FTIR analysis

To confirm the functional groups on PVBC microspheres, the ATR-FTIR spectra of the pristine PVBC and PDMAPMA-grafted microspheres were characterized, and were shown in Figure S3 (Supporting Information). Figure 3 shows the corresponding expanded-view FTIR spectra in a wavenumber range of 1800-1350 cm^{-1} of the above microspheres. As shown in Figure S3a, the main bands observed in the FTIR spectrum of the pristine PVBC microspheres include the stretching vibration of C=O bond ($\nu_{(c=o)}$) of EGDMA at 1720 cm^{-1}, the in-plane bending vibration of the CH_2Cl groups ($\delta_{(CH2\text{-}cl)}$) at 1261 cm^{-1}, the out-plane bending vibration of aromatic ring ($\gamma_{(C\text{-}H)}$) at 835 cm^{-1}, and the stretching vibrations of C-Cl bonds at 670 cm^{-1} ($\nu_{(C\text{-}Cl)}$) of PVBC.[56] The characteristic CH_2Cl and C-Cl peaks in the FTIR spectrum confirm the presence of abundant chloromethyl groups on the PVBC microspheres to cater for subsequent ATRP reaction of DMAPMA. As compared to the pristine PVBC microspheres, the successful grafting of PDMAPMA brushes on the PVBC microsphere surfaces can be deduced from the appearance of additional bands of the stretching vibration of amide I ($\nu_{(C=ONH)}$) at 1658 cm^{-1}, ,the bending vibration of amide II ($\delta_{(N\text{-}HC=O)}$) at1534 cm^{-1}, and the N-H stretching vibration ($\nu_{(N\text{-}H)}$) at 3380 cm^{-1} (Figs. 3b and 3c).[57] As observed closely from Figure 3, the relative intensity of the characteristic amide I, amide II and the asymmetric vibration of C=O (at 1612 cm^{-1}) peaks of PVBC-*g*-PDMAPMA2 surface from 6 h of ATRP reaction is much stronger than that of the PVBC-*g*-PDMAPMA1 surface from 2 h of ATRP reaction, indicating that the longer PDMAPMA brushes are grown from the PVBC microspheres upon increasing the ATRP reaction time.

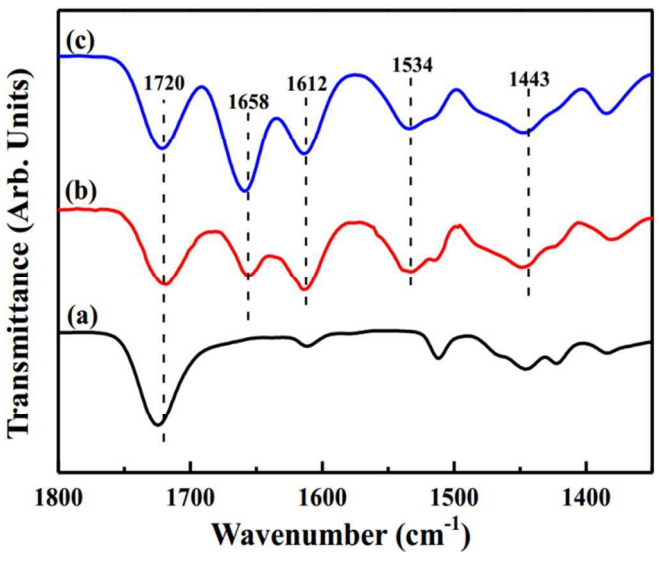

Figure 3 The expanded-view ATR-FTIR spectra in a wavenumber range of 1800 – 1350 cm^{-1}. of the surfaces of (a) the cross-linked PVBC microspheres, (b) the PVBC-*g*-PDMAPMA1 microspheres from 2 h of ATRP reaction, and (c) the PVBC-*g*-PDMAPMA2 microspheres from 6 h of ATRP reaction.

3.2.2 XPS characterization

The chemical compositions of the cross-linked PVBC microsphere surfaces before and after grafting of PDMAPMA brushes were also determined by XPS. Figure 4 shows the respective wide scan, C 1s, N 1s and Cl 2p core-level XPS spectra of the pristine and PDMAPMA-grafted PVBC microspheres. The C 1s core-level spectrum of the pristine PVBC microsphere surfaces can be curve-fitted into three peak components with binding energies (BEs) at 284.6, 286.3, and 288.6 eV, attributable to the C-H, C-Cl, and O=C-O species, respectively (Fig. 4b).[58] The C-Cl characteristic peak component is associated with the abundant chloromethyl groups on the PVBC surface, while the appearance of O=C-O species is ascribed to the cross-linker of EGDMA. The corresponding Cl 2p core-level spectrum with a spin-orbit-split doublet of Cl $2p_{3/2}$ (BE at 200 eV) and Cl $2p_{1/2}$ (BEs of at 201.7 eV) is consistent with the presence of the methyl chlorine species (Fig. 4c).[59] The additional peak component with BE at 197.8 eV in the Cl 2p core-level spectrum is probably ascribed to the radical anion of the chloromethyl groups during X-ray excitation in the XPS analysis chamber.[58] The [Cl]/[C] ratio, as determined from the sensitivity factor-corrected Cl 2p and C 1s core-level spectral area ratio, is around 0.031. The PVBC-*g*-PDMAPMA microspheres were synthesized via surface-initiated ATRP of DMAPAM by controlling the feed molar ratio of [DMAPMA (monomer)]:[CuCl (catalyst)]:[$CuCl_2$ (deactivator)]: [PMDETA (ligand)] at 100:1.0:0.1:2.0 for 2 and 6 h of reaction. Figures 4d-i show the wide scan, C 1s, N 1s and Cl 2p core-level XPS spectra for the PVBC-*g*-PDMAPMA microsphere surfaces from 2 and 6 h of ATRP reaction, respectively. For the PVBC-*g*-PDMAPMA1 surface from 2 h of ATRP reaction, an additional N 1s signal with BE at about 400 eV is clearly observed in the wide scan spectrum, as compared to that of the pristine PVBC microsphere, indicative of the successful grafting of PDMAPMA brushes (Fig. 4d). The [N]/[C] ratio, as determined from the sensitivity factor-corrected N 1s and C 1s spectral area ratio, is around 0.076, is far less than the theoretical ratio of 0.22 for the DMAPMA repeat unit structure, indicating that the thickness of the PDMAPMA brushes grafted onto the PVBC microspheres is less than 8 nm (the probing depth of XPS technique[58]). The curve-fitted C 1s core-level spectrum consists of four peak components of C-H (284.6 eV), C-N (285.5 eV), C-Cl/C-N^+ (286.2 eV), and O=C-NH (287.8 eV) species (Fig. 4e). The appearance of characteristic C-N and O=C-NH peaks of the DMAPMA molecules is consistent with successful grafting of PDMAPMA brushes on the PVBC microspheres. The N 1s core-level spectrum shows a predominant peak component with BE at 399.6, attributable to the neutral amine groups (>N-), and a minor peak component with BE at 402.8 eV, attributable to the positive-charged nitrogen (-N^+) species, respectively (Fig. 4f). The appearance of the N^+ species reveals a small degree of self-quaternization of the PDMAPMA chain by the dormant alkyl chloride at the chain ends from the ATRP process.[60] The persistence of Cl species (Cl $2p_{3/2}$ and Cl $2p_{1/2}$ doublet, Inset Fig 4f') is consistent with the fact that the ''living'' chain end from the ATRP process involves a dormant alkyl halide group, which can be re-activated to initiate the subsequent block copolymerization.

Upon prolonging the ATRP time to 6 h, the PDMAPMA–grafted PVBC surface shows a significant increase in the relative intensity of N 1s signal in the wide scan spectrum (Fig. 4g), as compared to that of the PVBC-g-PDMAPMA1 from 2 h of ATRP reaction. The area ratio of [N]/[C] at 0.158 is comparable to the theoretical value of the DMAPMA molecular structure, indicating that the thickness of the PDMAPMA brushes is larger than the probing depth of the XPS techniques (about 8 nm in an organic matrix[58]). The increase in the thickness of PDMAPMA brushes grafted on the microsphere surfaces with ATRP time is further confirmed by the the curve-fitted C 1s spectrum (Fig. 4h). The area ratio of [C-H]:[C-N]:[O=CNH] at 4.3:2.7:1.0 in the curve-fitted C 1s spectrum for the PVBC-*g*-PDMAPMA2 microspheres is close to the PDMAPMA chemical structure with theoretical component ratio of 4:3:1 (Fig. 4h). The small deviation in the peak component area ratio is ascribed to the appearance C-Cl/C-N^+ species (BE at 286.2 eV) owing to the occurrence of self-quaternization of the tertiary amino groups on the PDMAPMA chains. The degree of self-quaternization of the PDMAPMA chains seems to increase with the ATRP time, as the $[N^+]/[N_T]$ ratio after 6 h of ATRP reaction increases to around 7.3% from about 5.4% for 2 h of ATRP reaction (Fig. 4i). The above results are in good agreement with previous findings that surface-initiated ATRP is strongly dependent on the reaction time and that the thickness of the polymer brushes increases linearly with the polymerization time.[51]

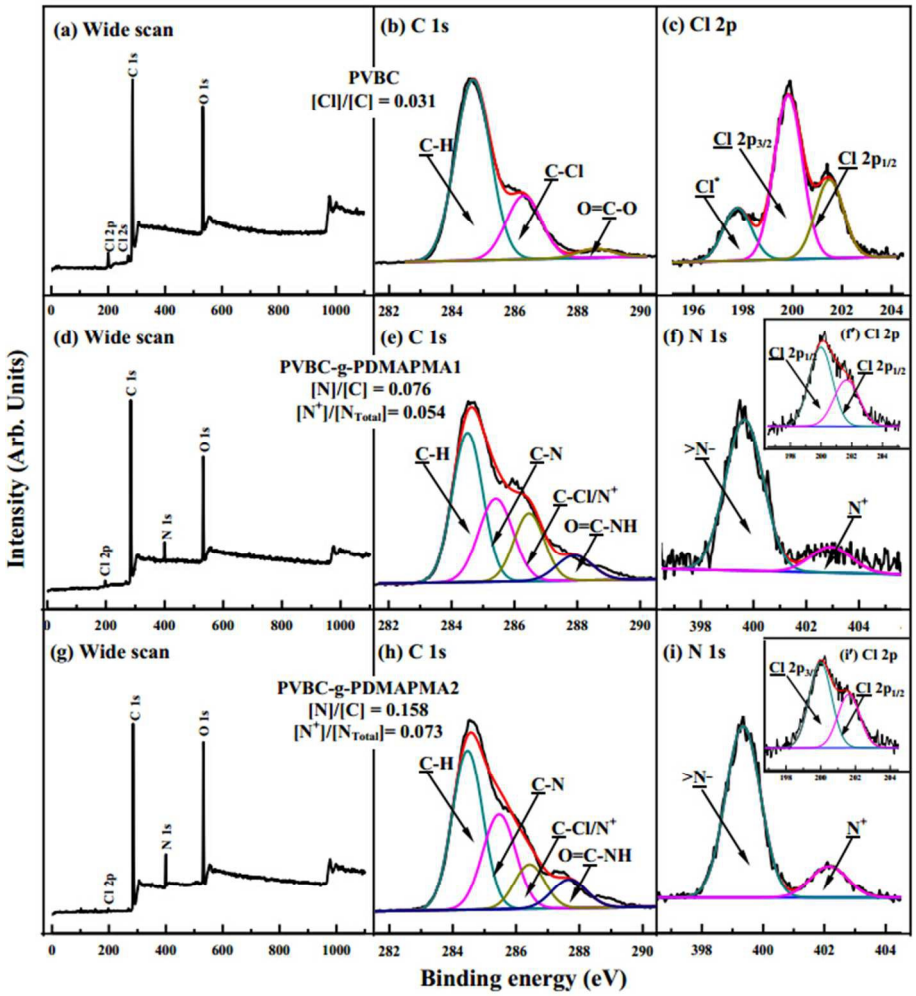

Figure 4 The wide scan, C 1s, Cl 2p and N 1s core-level XPS spectra of the surfaces of (a-c) the cross-linked PVBC microspheres, (d-f) the PVBC-*g*-PDMAPMA1 microspheres from 2 h of ATRP reaction, and (g-i) the PVBC-*g*-PDMAPMA2 microspheres from 6 h of ATRP reaction. Insets (f′) and (i′) show the corresponding Cl 2p core-level spectra of the PVBC-*g*-PDMAPMA microsphere surfaces.

3.3 *N*-alkylation of surface-grafted PDMAPMA brushes

To produce the polycationic chains containg quaternary ammonium groups, the pendent tertiary amino groups on the PDMAPMA brushes were directly quaternized by nucelophilic substitution reaction with bromoethane. The surface compositions of the quaternized PDMAPMA-grafted PVBC microsphere surfaces from 2 and 6 h of ATRP reaction were characterized by FTIR and XPS to ascertain the success of *N*-alkylation reaction.

3.3.1 FTIR analysis

The FTIR spectra of the quaternized PDMAPMA-grafted PVBC microspheres are shown in Figure S4 (Supporting Information). Figure 5 shows the expanded-view FTIR spectra of quaternized PDMAPMA-grafted PVBC microsphere surfaces from 2 and 6 h of ATRP reaction. After the quaternization reaction, an additional minor peak at 1480 cm^{-1}, attributable to the vibration stretching of $C\text{-}N^{+}$ ($\nu_{(C\text{-}N^{+})}$), is observed in the expanded-view FTIR spectra.[61] The peaks at 3398 and 1660 cm^{-1} in the FTIR spectra of the PVBC-*g*-PDMAPMA microspheres are the characteristic vibrations of quaternary nitrogen (Fig. S4).[62] Since bromoethane was used in the *N*-alkylation reaction, the wide peak in the range of 2955-2837 cm^{-1} (the main peak at 2934 cm^{-1}), attributable to the C-H antisymmetric and symmetric stretching in $-CH_3$ and $-CH_2$ groups (Fig. S4), suggests the successful addition of alkyl chains to the polymer.[63] The above results are consistent with the successful quaternization of the PDMAPMA chains grafted on the PVBC microsphere surfaces to produce the polycationic chains containing quaternary ammonium groups.

3.3.2 XPS analysis

Figure 6 of show the respective wide scan, N 1s and Br 3d core-level spectra of the quaternized PDMAPMA-grafted microsphere surfaces after 24 h of quaternization reaction. As compared to the wide scan spectra of the PVBC-*g*-PDMAPMA surfaces before *N*-alkylation, the appearance of three signals with BEs at about 69, 182, and

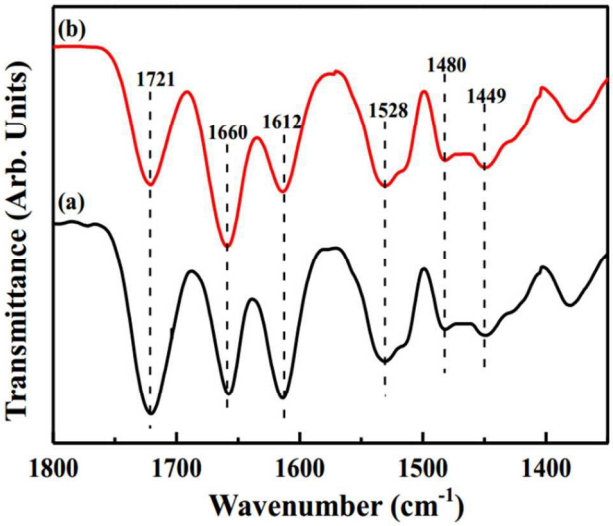

Figure 5 The expanded-view ATR-FTIR spectra in a wavenumber range of 1800 - 1350 cm^{-1} of the surfaces of (a) the PVBC-*g*-QPDMAPMA1 and (b) PVBC-*g*-QPDMAPMA2 microspheres.

255 eV, attributable to the Br 3d, Br 3p and Br 3s species, respectively, indicates the successful *N*-alkylation reaction of the PDMAPMA brushes by bromomethane (Figs. 6a and 6d). The curve-fitted N 1s core-level spectra consist of a minor peak component with BE at 399.4 eV, attributable to the neutral amine species, and a dominant peak component with BE at 402.6 eV, attributable to the positively-charged nitrogen ($-N^+$) species, respectively (Figs. 6b and 6e). The extent of quaternization for the tertiary amino groups of the PDMAPMA chains can be expressed as the $[N^+]/[N_{Total}]$ ratios, determined from the corresponding N^+ peak component and total nitrogen spectral area ratio within the probing depth of the XPS instruments. The $[N^+]/[N_{Total}]$ ratio for the PVBC-*g*-QPDMAPMA1 and PVBC-*g*-QPDMAPMA2 surfaces are about 0.85 and 0.74, respectively, after 24 h of quaternization reaction. The $[N^+]/[N_{Total}]$ ratios of the PVBC-g-QPDMAPMA surfaces are significantly higher than those of the corresponding PVBC-*g*-PDMAPMA surfaces, indicating that the tertiary amino groups in the PDMAPMA chains are almost completely *N*-alkylated after 24 h of quaternization reaction. This result is further confirmed by the [Br]/[N] ratio of 0.94 and 0.82 for the PVBC-*g*-QPDMAPMA1 and PVBC-*g*-QPDMAPMA2 surfaces, respectively (Figs. 6c and 6f). On the other hand, the quaternization degree of the PVBC-*g*-QPDMAPMA2 surface from 6 h of ATRP reaction is slightly lower than that of the PVBC-*g*-QPDMAPMA1 surface, which is probably associated with the long PDMAPMA brushes on the former microsphere surfaces. The longer of the PDMAPMA brushes grafted on the PVBC microsphere surfaces, the more difficult for the bromomethane to attack the deep tertiary amino groups on the PDMAPMA chains for nucelophilic substitution reaction. However, the surface density of the quaternary ammonium groups on the PVBC-*g*-QPDMAPMA2 surface is virtually much higher than those on the PVBC-*g*-QPDMAPMA1 surface on the basis of the grafting density of PDMAPMA brushes (Fig. 2) and the quaternization ratio. Thus, the polycationic QPDMAPMA chains have been successfully grafted onto the PVBC microspheres with abundant quaternary ammonium groups.

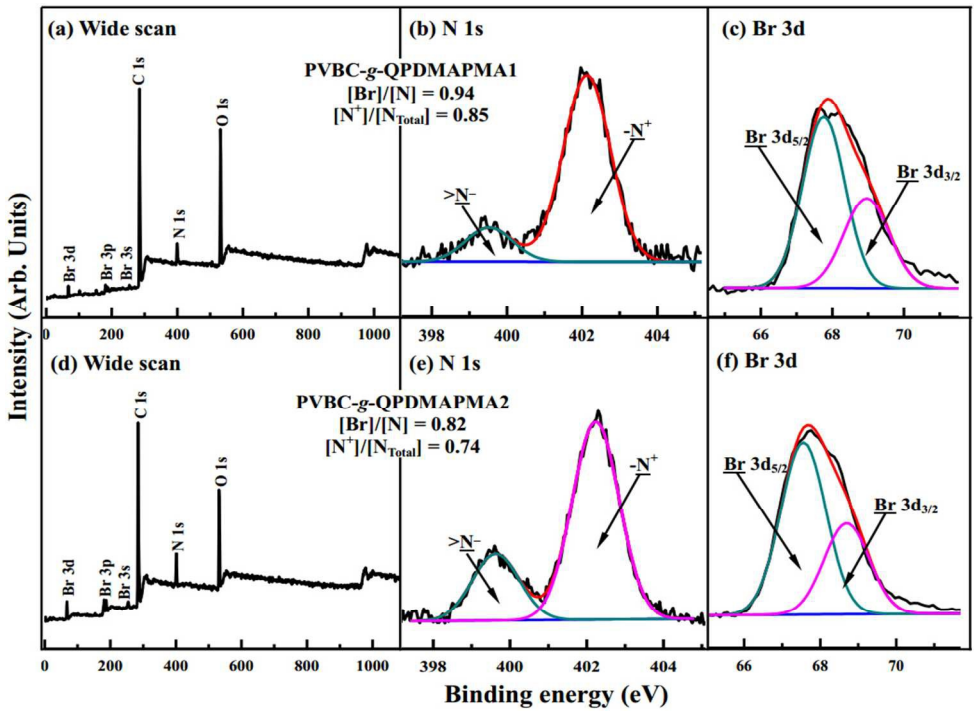

Figure 6 The wide scan, N 1s and Br 3d core-level XPS spectra of the surfaces of (a-c) the PVBC-*g*-QPDMAPMA1 and (d-e) the PVBC-*g*-QPDMAPMA2 microspheres.

3.4 Adsorption features of the quaternized PDMAPMA-grafted microspheres

In this study, the phenol-contaminated aqueous solution was used to evaluate the adsorption behavior of the quaternized PDMAPMA-grafted PVBC microspheres. Different factors, such as the grafting time, solution pH and ionic strength of co-existing salts, were investigated to determine their effect on the adsorption capacity of the synthesized adsorbents. The adsorption kinetics, adsorption isotherms and thermodynamic parameters of the phenol for the quaternized PDAMPMA-grafted microspheres were also determined.

3.4.1 Effect of grafting yield

As shown in Figure 2, the grafting density of the PDMAPMA brushes on the microsphere surfaces increase linearly with grafting time. The PDMAPMA brushes obtained at different grafting time were quaternized by bromomethane for 24 h for phenol adsorption tests under same experimental conditions. The results of the adsorption capacity of phenol with different grafting yield are shown in Figure 8a. It is clearly observed that the phenol adsorption capacity increases linearly with grafting yield before reaching the value of about 7.5%.. The results are understandable as higher grafting yield can provide more anchor sites (i.e. quaternary ammonium ions) for adsorbates. The increase in adsorption capacity slows down (from 1.12 to 1.66 mmol·g^{-1} from about 7.5% to 15.1% (Fig. 7a), while the grafting density of increase linearly from 0.44 to 0.89 mmol·g^{-1} (Fig. 2), indicating that excess long polymeric chains do not show any significant increase in the adsorption capacity of phenol on the quaternized PDMAPMA-grafted microspheres. Phenol may be difficult to diffuse into the long and dense polycationic QPDMAPMA chains grafted on the PVBC microsphere surfaces. These results are consistent well with previous finding that excessively prolonging grafting time have little contribution to the enhanced sorption capability of adsorbent synthesized by surface-initiated ATRP.[54, 64] To achieve the high adsorption capacity, the grafting yield is controlled at 15.1% (from 6 h of ATRP time) to prepare the quaternized PDMAPMA-grafted PVBC microspheres, i.e. PVBC-*g*-QPDMAPMA, used in the following sorption experiments.

3.4.2 Effect of solution pH

Solution pH has been widely accepted to affect the adsorption of adsorbates if the adsorbate molecules or adsorbent surface are ionizable.[64] Phenol, also known as carbolic acid, is a weak acid with pKa value of about 9.95 due to stabilization of the conjugate base through resonance in the aromatic ring, and it exists as anionic species at the pH studied. At a proper pH values, phenol is ionized to give the phenolate anion $C_6H_5O^-$ (i.e. phenoxide) as follows:[65]

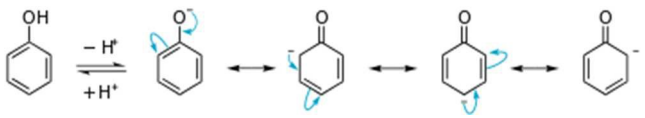

Therefore, the adsorption of phenol on the quaternized microspheres is dominated by an ion exchange process. The effect of solution pH on the phenol adsorption onto the PVBC-*g*-QPDMAPMA2 microspheres is shown in Figure 7b. The solution pH values have little effect on the adsorption capacity of phenol onto the quaternized microspheres within a pH range of 3 - 9, as the adsorbed amounts of phenol seems to remain constant with the increase in pH values from 3 to 9. However, the adsorption capacity of phenol shows a slight increase (approximately 5%) upon with increasing pH value more than 10. The relatively higher adsorption capacity at high pH is ascribed to the ionization of phenol to generate more phenolate anions, and thus resulting in the enhanced phenol adsorption via the electrostatic attraction between the anionic phenol and the quaternary ammonium cations on the quaternized PDMAPMA chains.

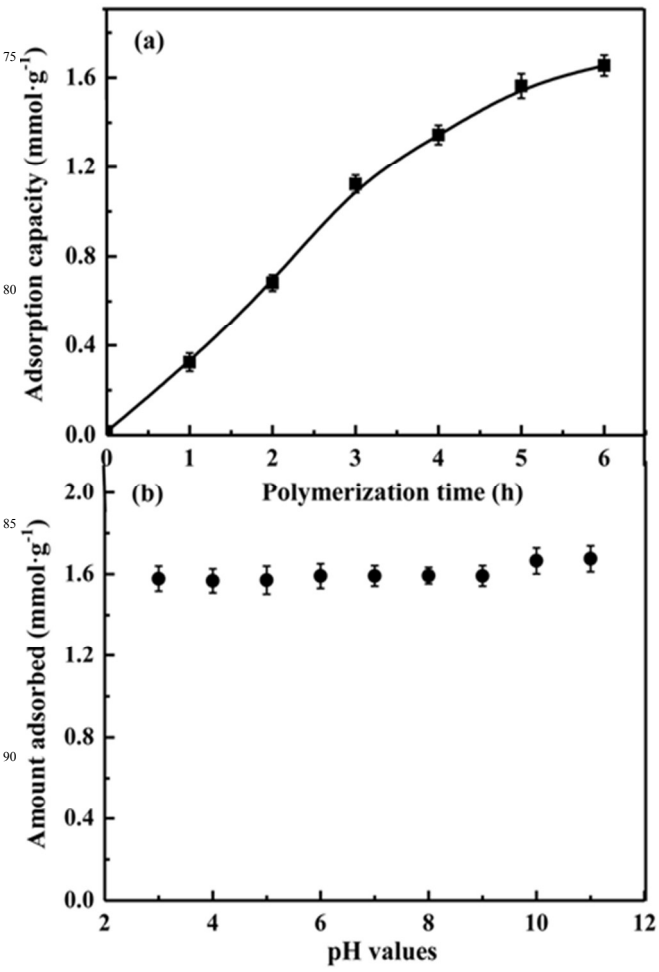

Figure 7 (a) The dependence of adsorption capacity of phenol on the ATRP time for the quaternized PDMAPMA-grafted microspheres, (b) the effect of solution pH values on the adsorption amount of phenol on the PVBC-*g*-QPDMAPMA2 microspheres. Experimental conditions: the initial phenol concentration C_0 = 2.13 mmol·L^{-1}·(i.e. 200 mg·L^{-1}), temperature T = 298.15 K, sorbent dosage m = 0.1 g, v = 100 mL, and adsorption time t = 24 h.

Most adsorbents have low adsorption capacity for phenol at high solution pH due to the interactions between phenol and adsorbents via hydrogen bonds,[66, 67] while a strongly basic anion-exchange *N*-butylimidazolium-modified resin MCl (quaternary ammonium) exhibits stable adsorption for phenol at a high pH value of 11.[68] It is evident that solution pH has little effect on the adsorption of phenol on the PVBC-*g*-QPDMAPMA2 microspheres, and this adsorbent can remove the phenol from aqueous solution efficiently in a wide pH range. Therefore, the solution pH value for the usage of quaternized PVBC microspheres is selected as 6.5 for the purpose of better control of adsorption tests, as well as the comparison with the previously-reported adsorbents for phenol removal. The subsequent sorption kinetics, sorption isotherms and thermodynamic tests are conducted with solution pH 6.5.

3.4.3 Sorption kinetics

The interaction of anionic phenol with the quaternary ammonium groups is highly desired to occur for the rapid removal of the phenol contaminants from aqueous solutions. Thus, the phenol sorption kinetics onto the quaternized PDMAPMA-grafted microspheres was investigated at pH 6.5. Figure 8 shows the sorption kinetics of phenol on the quaternized microspheres. With increasing the adsorption time, the adsorption amounts of phenol on the quaternized microspheres undergo an exponential increase at the first 20 min, and increase slowly due to the less active sorption sites available**.** The phenol adsorption on the quaternized microsphere is a very rapid process, and the adsorbed amounts during the initially 20 min of period are estimated to contribute approximately 90% of the total adsorption amounts. As a consequence, the adsorption equilibrium of phenol on the quaternized microspheres can be achieved within 60 min with an equilibrium sorption amount of 1.63 mmol·g^{-1}. As shown in Table S1 (Supporting Information), most of activated carbon adsorbents require more than 24 h to achieve the sorption equilibrium[67] and the polymeric adsorbents take at least 7 h to reach the sorption equilibrium.[14] Generally, when phenol is adsorbed on the porous adsorbents, the difficulty in the diffusion of phenol into the intraparticle pores makes the adsorption a very slow process. In this study, the long quaternized PDMAPMA chains were grafted onto the PVBC microsphere surface, and the phenol adsorption takes place only on the microsphere surface, thus resulting in a rapid adsorption.

To further understand the adsorption kinetics, the kinetic data of the phenol adsorption on the PVBC-*g*-QPDMAPMA2 microspheres are fitted by using the pseudo-first-order (PFO) and pseudo-second-order (PSO) kinetic models. The PFO and PSO kinetic models are expressed as the following Equations 5 and 6, respectively:[69]

$$q_t = q_{\max}(1 - e^{k_f \cdot t}) \quad (5)$$

$$q_t = \frac{(q_{\max}^2 \cdot k_s \cdot t)}{(1 + q_{\max} \cdot k_s \cdot t)} \quad (6)$$

where k_f is the rate constant of pseudo-first-order adsorption (min^{-1}), k_s is the rate constant of the pseudo-second-order reaction (gmmol^{-1}min^{-1}), q_t is the adsorbed amount at time t (min), and q_{max} denotes the amount adsorbed at equilibrium, both in mmol·g^{-1}. The values of k_f , k_s and q_{max} are all obtained by nonlinear fitting, and the fitted parameters are summarized in Table 1. It is widely recognized that the PFO and PSO kinetic models are established by considering the external film diffusion, intraparticle diffusion, and interaction step in the total process of adsorption.[69] Either of the above steps can control the adsorption rate of the adsorbates on the adsorbents. For the phenol adsorption on the quaternized microspheres, the external film diffusion has been eliminated by continuous stirring at 150 rpm during the adsorption process, thus the controlling-step of the phenol sorption rate is readily recognized as the intraparticle diffusion or an interaction step. As shown in Table 1, the adsorption kinetic data of the PVBC-*g*-QPDMAPMA2 microspheres are well represented by the PFO model with the chi square (χ^2) as low as 0.00159. Because the PFO model is based on the assumption that the rate-determining step may be chemisorption promoted by covalent forces through the electron exchange or valency forces through electron sharing between the adsorbents and the adosrbates, hence, this result suggests that the electrostatic interaction of anionic phenolate with quaternary ammonium groups of the polycationic QPDMAPMA brushes, as well as the weak hydrogen bonding derived from the interaction of tertiary amino groups and phenol speices, may dominate as the rate-limiting step of the phenol adsorption, and no solution mass transfer is involved in the adsorption process, The calculated q_{max} values of 1.65 mmol·g^{-1} (i.e. 155 mg·g^{-1}) by the PFO model are perfectly matched with the experimental values of 1.63 mmol·g^{-1} for the PVBC-*g*-QPDMAPMA2 microspheres. Hence, the quaternized PDMAPMA-grafted microspheres are a potentially useful adsorbent to remove phenol in a much shorter process time.

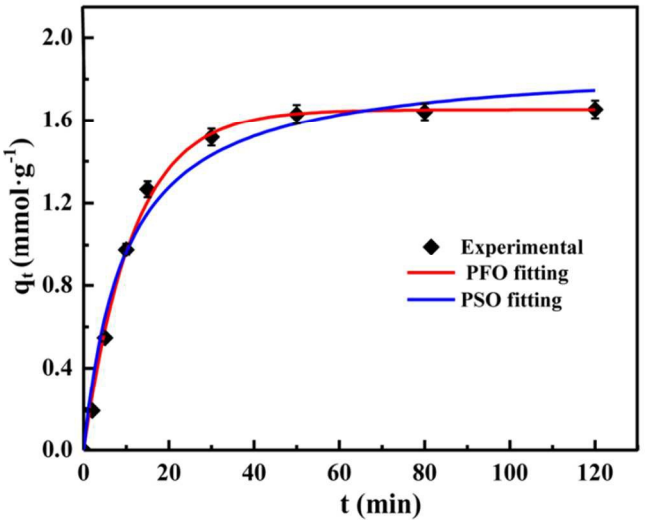

Figure 8 Adsorption kinetics of phenol on the PVBC-*g*-QPDMAPMA2 microspheres. Experimental conditions: C_0 = 2.13 mmol·L^{-1} (i.e. 200 mg·L^{-1}), T = 298.15 K, m = 0.1 g, v = 100 mL, and initial pH =6.5.

Table 1. Kinetic parameters for the adsorption of phenol on the PVBC-*g*-QPDMAPMA2 microspheres at a temperature of 298.15K

Models	Model parameters				
	k_f (min^{-1})	k_s ($gmmol^{-1}min^{-1}$)	q_{max} ($mmolg^{-1}$)	χ^2	R^2
PFO[a]	0.088	--	1.65	0.0016	0.996
PSO[b]	--	0.056	1.89	0.0089	0.979

[a] PFO refers to the pseudo-first-order kinetic model.
[b] PSO corresponds to the pseudo-second-order kinetic model

3.4.4 Sorption isotherms

Adsorption equilibrium isotherm is critical to determine the maximum adsorption capacity for the evaluation of adsorption efficiency of adsorbents. Figure 9 shows the adsorption isotherms of phenol on the PVBC-*g*-QPDMAPMA2 surfaces at 298.15, 308.15, 318.15, and 328.5 K, respectively. It is clearly observed that increasing equilibrium concentration and decreasing temperature favor the phenol adsorption on the quaternized microspheres. The maximum adsorption capacity of phenol reaches as high as about 2.02 mmol·g^{-1} (i.e. 190 mg·g^{-1}) at the initial phenol concentration of about 5.31 mmol·L^{-1} (i.e. 500 mg·g^{-1}) and 298.15 K. The adsorption capacities of phenol on the quaternized microspheres increase very fast with increasing equilibrium concentration of phenol solution, and the high sorption amount can be achieved at relatively low concentrations. The adsorbed amounts of phenol almost remain constant with further increasing the initial phenol concentration above 1.60 mmol·L^{-1} (i.e. 150 mg·g^{-1}), indicative of a possible monolayer adsorption of phenol on the quaternized PVBC-*g*-QPDMAPMA2 microspheres. On the other hand, the molecular phenol species rather than phenolate species dominate at solution pH of 6.5, and the phenol sorption undergoes a notable decrease with the rise in the temperature. This result is in good agreement with the fact that the adsorption of molecular phenol species on the quaternized microsphere is exothermic under acidic pH conditions. Similar results have been reported in previous studies, in which phenols are adsorbed on the *N*-methylacetamide-modified hypercrosslinked resin HJ-Z01,[14] *N*-butylimidazolium functionalized anion-exchange resin MCl,[68] and aminated polymeric adsorbents MN-100 and MN-150,[70] at acidic pH.

To obtain the information on the adsorption equilibrium and maximum adsorption capacities in a more quantitative manner, the experimental data of phenol adsorption on the quaternized microspheres are modeled by using the Langmuir, Freundlich and Temkin isotherms. These theoretical isotherm models enable the analysis of the relative affinity of the quaternized microspheres for the phenol and allow to correlate the adsorption data with the surface properties of the quaternized PDMAPMA-grafted microspheres. The Langmuir isotherm model assumes surface homogeneity, such as equal adsorption activation energy of each adsorbed molecule, monolayer surface coverage of adsorbate, and no interaction between the adsorbed molecules, whereas the Freundlich model is derived by assuming a heterogeneous surface with a non-uniform distribution of heat of adsorption over the surface and is thus expressed as multilayer adsorption. On the other hand, the Temkin model makes assumption that the decline of the sorption heat as a function of temperature is linear rather than logarithmic. The Langmuir, Freundlich, and Temkin isotherm models are expressed as the following equations 7, 8 and 9 respectively:

$$q_e = \frac{K_L \cdot q_{\max} \cdot C_e}{(1 + K_L \cdot C_e)} \quad (7)$$

$$q_e = K_F \cdot C_e^{1/n} \quad (8)$$

$$q_e = \frac{RT}{B_T} \ln A_T + \frac{RT}{B_T} \ln C_e \quad (9)$$

where q_{max} is the maximum adsorption capacity (mmol·g^{-1}), K_L represents the adsorption equilibrium constant (mmol·L^{-1}), C_e is the equilibrium concentration of phenol in the solution (mmol·L^{-1}), q_e corresponds to the adsorbed amount at equilibrium (mmol·g^{-1}), K_F is an empirical constant representing the adsorption capacity ($mmol^{(1-1/n)} \cdot L^{1/n} \cdot g^{-1}$) and n is the Freundlich constant depicting the adsorption intensity, A_T is the equilibrium binding constant corresponding to the maximum binding energy (L·g^{-1}), B_T is the Temkin constant related to the heat of sorption (kJ·mol^{-1}), and R is the gas constant (8.314×10^{-3} kJ·mol^{-1}·K^{-1}), T is the absolute temperature (K).

Table 2 The regression parameters obtained using Langmuir, Freundlich and Temkin isotherms for the phenol adsorption data on the PVBC-*g*-QPDMAPMA microspheres at four different temperatures.

Model	Fitted Parameters	Temperature (K)			
		298.15	308.15	318.15	328.15
Langmuir	q_{max} (mmol·g^{-1})	2.23	2.10	2.04	1.88
	K_L (L·mmol^{-1})	3.59	3.18	2.70	2.33
	χ^2	0.0037	0.0027	0.0023	3.011E^{-4}
	R^2	0.991	0.994	0.993	0.999
Freundlich	n	4.27	4.14	3.97	3.77
	K_F (mmol$^{1-1/n}$L$^{1/n}$·g^{-1})	1.63	1.50	1.40	1.25
	χ^2	0.022	0.016	0.015	0.0071
	R^2	0.949	0.958	0.954	0.975
Temkin	K_T (L·mmol^{-1})	63.77	53.34	40.52	32.87
	b_T	6.21	6.46	6.44	6.83
	χ^2	0.013	0.0091	0.0089	0.0031
	R^2	0.969	0.976	0.974	0.989

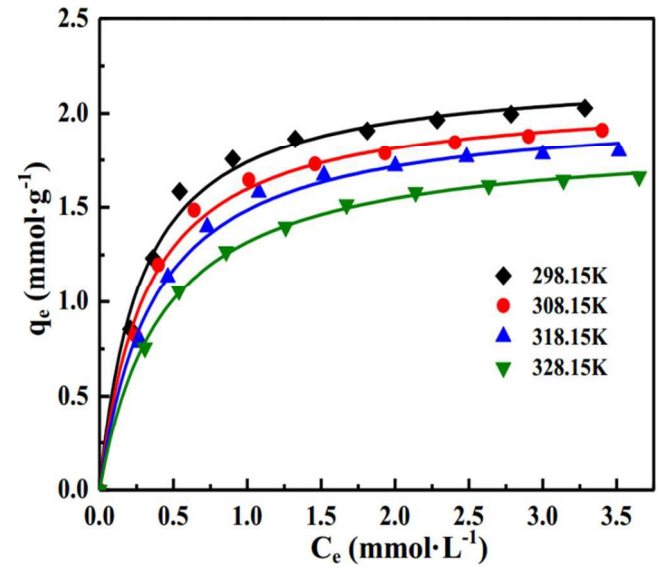

Figure 9 Langmuir-fitted adsorption isotherms of phenol on the PVBC-*g*-QPDMAPMA2 microspheres at 298.15, 308.15, 318.15, and 328.15 K. Experimental conditions: C_0 = 1.05 – 5.31 mmol·L^{-1} (i.e. 100 - 500 mg·L^{-1}), T = 298.15 K, m = 0.1 g, v = 100 mL, t = 24 h, and initial pH =6.5.

The nonlinear fitting were conducted for the above three isotherm models to depict the equilibrium adsorption process of phenol on the quaternized microspheres, and the optimal parameters of each model are summarized in Table 3. The fitted lines derived from the modeling of Langmuir, Freundlich and Temkin isotherms are illustrated in Figure 10, Figure S5 and Figure S6 (Supplementary Information), respectively. When comparing the values of chi square (χ^2) for each isotherm model (Table 2), the Langmuir model represents a better fit for the experimental data than the Freundlich and Temkin models in all cases for the adsorption of phenol. This reflects that the surface of the quaternized PDMAPMA-grafted microspheres is made up of homogeneous adsorption sites, and that a monolayer adsorption of phenol may take place on the homogenous quaternized microsphere surfaces. According to the Langmuir fitting results, the maximum sorption capacities of phenol on the quternized PVBC-*g*-PDMAPMA2 microspheres at 298.15, 308.15, 318.15 and 328.15 K are 2.23, 2.10, 2.04, 1.88 mmol·g^{-1}, respectively. Some other adsorbents have been reported to remove phenol from aqueous solution (Table S1), and the maximum sorption capacities are 1.09 - 2.53 mmol·g^{-1} (pH = 4.0 - 7.0) on activated carbon-based adsorbents,[10, 11, 67, 71] 0.12 mmol·g^{-1} (pH = 5.8) on modified natural red clay,[19] 1.43 – 2.46 mmol·g^{-1} (pH = 6.0 – 7.5) on the polymeric adsorbents,[14, 29, 70] 1.52 mmol·g^{-1} (pH = 8.0) on the fly ash,[15] 0.99 mmol·g^{-1} (pH = 11) on the *N*-butylimidazolium-grafted ion-exchange resins (MCl),[68] 1.97 mmol·g^{-1} (pH = 7.0) on the nitrogen-functionalized magnetic ordered carbon (N-Fe/OMC),[72] 1.0 mmol·g^{-1} (pH = 6.0 – 7.0) on the sewage sludge,[20] and 1.15 mmol·g^{-1} (pH = 7.0) on the chitosan-calcium alginate blended beads.[12] Among these previously-reported adsorbents, only the granular activated carbon (2.53 mmol·g^{-1} at pH 5.5) and aminated polymeric resin MN-150 (2.46 mmol·g^{-1} at pH 6.5) have higher adsorption

capacity for phenol than the quaternized PDMAPMA-grafted PVBC microspheres, however, the two adsorbents requires 96 and 72 h, respectively, to achieve the adsorption equilibrium. Therefore, the quaternized PDMAPMA-grafted microspheres have competitive advantages of higher adsorption capacity and faster adsorption rate for the removal of phenol from the phenol-contaminated aqueous solutions.

3.4.5 Adsorption thermodynamics

Adsorption thermodynamic parameters provide in-depth information on inherent energetic changes that are associated with adsorption, including adsorption enthalpy (ΔH, kJ·mol^{-1}), adsorption Gibbs free energy (ΔG, kJ·mol^{-1}), and adsorption entropy (ΔS, kJ·mol^{-1}·K).[10, 73] Among them, ΔG is a fundamental criterion to judge the adsorption spontaneity, and an adsorption can takes place spontaneously at a given temperature if the value of ΔG is negative. ΔH is defined as the adsorption heat associated with the interaction between the adsorbent and the adsorbate, and it represents endothermic or exothermic feature of an adsorption process. ΔS is used to depict the degree of chaos of a given system. A positive value of ΔS reflects an increasing randomness at the solid/liquid interface during the adsorption process, while the negative counterpart implies a more ordered system after adsorption. The sorption isotherms obtained at different temperatures can be used to estimate the thermodynamic parameters using the following Van′t Hoff equations if the enthalpy change ΔH^0 is constant in the studied temperature range:

$$\ln K_L = -\frac{\Delta H^0}{RT} + \frac{\Delta S^0}{R} \quad (10)$$

where K_L is the adsorption equilibrium constant obtained from Langmuir isotherms at different temperatures, R is the universal gas constant (8.314 J·mol^{-1}·K^{-1}), and T is absolute temperature (K).

According to equation 10, a linear plot is regressed to obtain the relationship between $\ln K_L$ and $1/T$. The standard adsorption enthalpy (ΔH^0) and entropy (ΔS^0) for the adsorption process of phenol on the quaternized microspheres can be obtained in terms of the slope and intercept of the plot, as shown in Figure S7 (Supporting Information). The values of Gibbs free energy ΔG^0 can be calculated from the following equation:

$$\Delta G^0 = \Delta H^0 - T\Delta S^0 \quad (11)$$

The values of thermodynamic parameters in the studied temperature range are summarized in Table 3**.** The negative values of ΔG^0 indicate that the adsorption process of the phenol on the quaternized PDMAPMA-grafted PVBC microspheres is spontaneous. The increase in the negative ΔG^0 values with increasing temperature indicates that the adsorption is more favorable at lower temperature. The standard enthalpy and entropy changes of adsorption derived from Figure S7 (Supporting Information) are calculated to be -11.27 kJ·mol^{-1} and -27.09 J·mol^{-1}·K^{-1}, respectively, with a correlation coefficient of 0.998. The negative value of ΔH^0 suggests that the adsorption process of phenol on the quaternized microspheres is exothermic. This result is consistent with the previous finding that the adsorption on the quaternary ammonium salts-containing adsorbents is an exothermic process.[74] The negative value of ΔS^0 reflects the ordered arrangement of the system after the adsorption, indicating that the PVBC-*g*-PDMAPMA2 adsorbent does not undergo significant changes in its structure during the adsorption process, enabling the reuse of the quaternized microspheres in repetitive adsorption-desorption cycles.

3.4.6 Salt effect on the phenol adsorption of quaternized microspheres

To study the effect of various salts (or ionic strength) on the quaternized PDMAPMA-grafted microspheres, individual salt of NaCl, $NaNO_3$ and EDTA with the concentration range of 0 – 0.20 mol·L^{-1} was treated with phenol solution of 2.13 mmol·L^{-1} (i.e. 200 mg·L^{-1}). Figure 10 shows the effect of various salts of NaCl, $NaNO_3$ and EDTA on the adsorption amounts of phenol on the quaternized PVBC-*g*-QPDMAPMA2 microsphere surfaces. As for the inorganic salts of NaCl and $NaNO_3$, the adsorption amount of phenol exhibits a noticeable increase with the increasing the concentration (ionic strength) of either NaCl or $NaNO_3$ (Fig. 10a), as the adsorption capacity of phenol on the quatnerized microspheres increases from about 1.66 mmol·g^{-1} in deionized water to 1.77 mmol·g^{-1} and 1.81 mmol·g^{-1} in a 0.2 mol·L^{-1} $NaNO_3$ or NaCl solution, respectively. The increase in phenol adsorption on the quaternized microspheres with increasing salt concentration (ionic strength) is ascribed to the salting-out effect. When a non-electrolyte is introduced to an electrolyte, salting-out effect can exert an effect on the adsorption process by lowering the solubility of the non-electrolyte. The salting-out effect on the adsorption process is generally involved the following process:[75] the salts of NaCl and $NaNO_3$ dissociate to produce monovalent ions (i.e. Na^+, Cl^- and NO_3^-) in aqueous solution, and these ions, especially for cationic Na^+, tightly bind free water molecules to form well-organized ionic atmosphere. Thus, the volume of the aqueous solution undergoes a macroscopic decrease by a well-known electrostriction process. These hydrated ions are not able to freely dissolve into the non-ionic phenol, nor do they possess the ability to dissolve the phenol in the solution. Hence, only a smaller number of water molecules in their free form are available to accommodate the phenol molecules upon increasing the salt amount. Moreover, the salt effect of NaCl appears to be more pronounced than that of $NaNO_3$ on the phenol adsorption, because the NO_3^- ions produces a salting-in effect and the Cl^- ions a salting-out effect.[76] Moreover, the radius of hydrated Cl^- (1.95 Å) is smaller than that of the hydrated NO_3^- (3.40 Å).[77] Take together, the increase in the ionic strength of the solution by adding salts of NaCl and $NaNO_3$ results in the reduction of phenol solubility in aqueous solution. The lower adsorbate solubility in aqueous solution, the easier for the adsorbate to adsorb on the adsorbents.[78] Therefore, the salt effect of NaCl and $NaNO_3$ facilitates the adsorption of phenol on the quaternized microspheres.

Table 3. Thermodynamic parameters according to the Van't Hoff equation for the adsorption of phenol on the PVBC-*g*-QPDMAPMA2 microspheres

Temperature (K)	ΔH^o (kJ·mol^{-1})	ΔS^o (J·mol^{-1}· K^{-1})	ΔG^o (kJ·mol^{-1})	R^2
298.15	-11.27	-27.09	-3.19	0.998
308.15			-2.92	
318.15			-2.65	
328.15			-2.38	

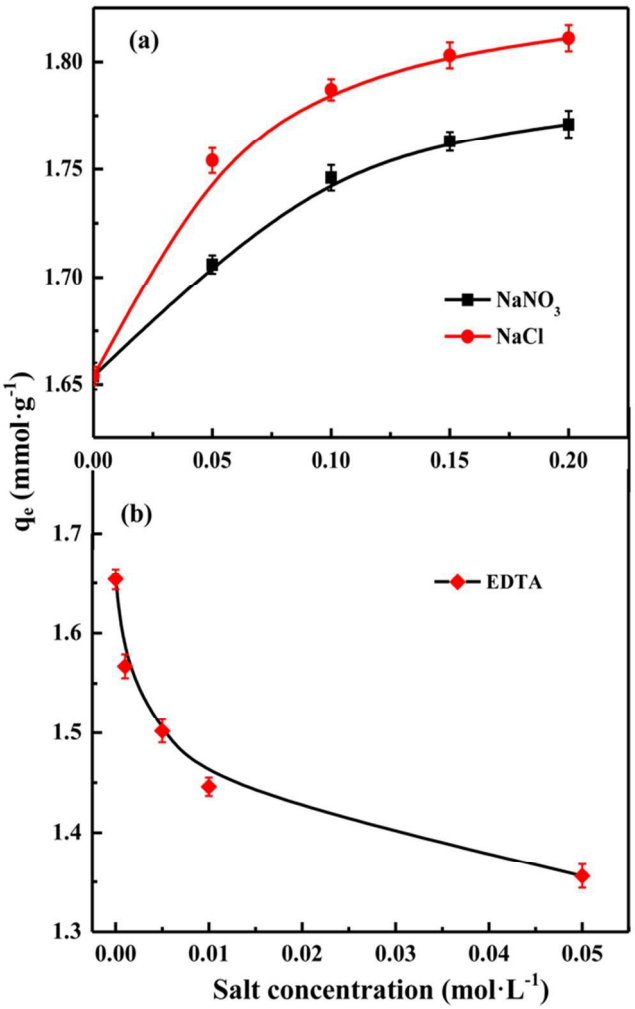

Figure 10 The effect of (a) NaCl and $NaNO_3$ and (b) EDTA on the adsorption of phenol on the PVBC-g-QPDMAPMA2 microspheres. Experimental conditions: C_0 =2.13 mmol·L^{-1} (i.e. 200 mg·L^{-1}), T = 298.15 K, m = 0.1 g, v = 100 mL, salt concentration C_{salt} = 0 ~ 0.20 mol·L^{-1}, EDTA concentration C_{EDTA} = 0 ~ 0.05 mol·L^{-1}, t = 24 h, and initial pH =6.5.

However, a significant difference of salt effect on the phenol adsorption can be distinguished from the organic EDTA with the inorganic salts of NaCl and $NaNO_3$. The effect of the concentration of EDTA on the sorption amount of phenol on the quaternized PDMAPMA-grafted microspheres is shown in the Figure 10b. With increasing the concentration (ionic strength) of EDTA in a range of 0.005 – 0.05 mol·L^{-1}, the adsorption amount of phenol on the quaternized PVBC-*g*-QPDMAPMA2 microspheres undergoes a gradual decrease to about 1.36 mmol·g^{-1} (Fig. 10b). The opposite tendency of salt effect by organic EDTA to that of the inorganic salts of NaCl and $NaNO_3$ is attributed the complexation of phenol by EDTA. The presence of tetra-carboxylic groups in the EDTA molecular structures makes it readily to tightly bind the phenol via hydrogen bonding, and thus retarding the diffusion of phenol in the adsorption process. Therefore, the adsorption of phenol by the EDTA effect is favorable to occur under the low-concentration experiment.

3.4.7 Regeneration of the quaternized PDMAPMA-grafted microspheres

In light of the environment-benign, sustainable and economical expectation of adsorbents, the regeneration features of the adsorbents for repeatable use is one of the most important aspects to evaluate the adsorbent efficiency for practical applications. Based on the fact the abundant quaternary ammonium groups (-N$^+$) and the secondary amine (-NH-) groups in the quaternized PDMAPMA chains are demonstrated to act as adsorption sites for phenol, the adsorption of phenol on the PVBC-*g*-QPDMAPMA2 surfaces via electrostatic interactions and hydrogen bonding may be a reversible adsorption process. The phenol loaded on the quaternized PDMAPMA chains can be possibly recovered by anionic exchange with hydroxyl groups (-OH). Thus, a 0.1 mol·L^{-1} NaOH solution was used to conduct desorption tests for the regeneration of the quaternized microspheres. The adsorption and desorption profiles of phenol on the PVBC-*g*-QPDMAPMA2 microspheres from five cycles are illustrated in Figure 11. Although the desorption efficiency of phenol on the quaternized microsphere undergoes a slight decrease from around 97% for the first run to about 88% after five cycles, its value still remain fairly high for the removal of phenol from aqueous solution. Similarly, the adsorption capacity of phenol decreases from about

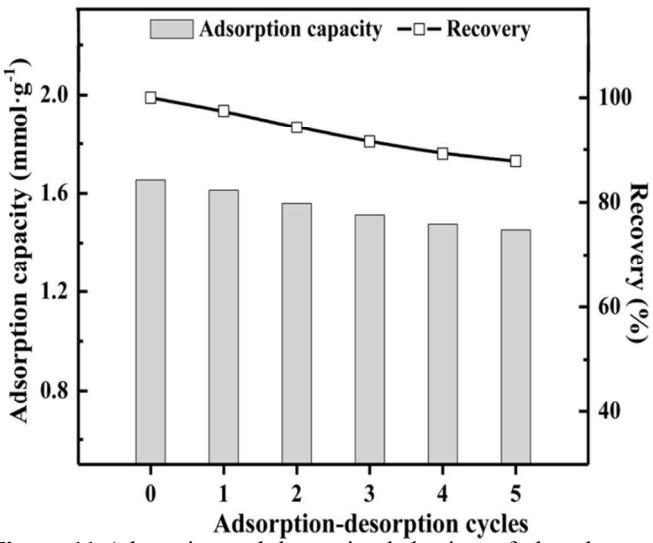

Figure 11 Adsorption and desorption behaviors of phenol on the PVBC-g-QPDMAPMA2 microspheres upon five cycles. Sorption experimental conditions: C_0 = 2.13 mmol·L^{-1} (i.e. 200 mg·L^{-1}), T = 298.15 K, m = 0.1 g, v = 100 mL, t = 24 h, and initial pH =6.5. Desorption experimental conditions: m = 0.1 g, T = 298.15 K, v = 100 mL, C_{NaOH} = 0.1 mol·L^{-1}, t = 2 h.

1.66 mmol·g^{-1} to about 1.45 mmol·g^{-1} from five cycles. The slight decrease in the removal efficiency of phenol removal after five cycles is possibly ascribed to the formation of robust chemical bonds between phenol and the polycationic PDMAPMA chains, which cannot be completely released from the adsorptive sites in the desorption process.

3.5 Adsorption Mechanisms

Taking into account of the surface features of the quaternized microspheres, three types of active l groups on the polycationic PDMAPMA brushes are probably involved in the phenol adsorption process: the quaternary ammonium groups (-N$^+$), the residual tertiary amines after *N*-alkylation, and the secondary amines of PDMAPMA chains. Thus, two postulated mechanisms of the phenol adsorption of on the quaternized PVBC-*g*-QPDMAPMA microspheres are virtually considered: the ion-exchange via electrostatic interactions and the hydrogen-binding formation. The schematic diagrams to illustrate the interactions of phenol with different active groups are shown in Figure S8 (Supporting Information). As the surface-initiated ATRP reaction of DMAPMA produces a high density of the grafting polymer chains on the microsphere surfaces and most pendent tertiary amino groups are converted into quaternary ammonium groups, it is predictable that the phenol has a huge opportunity to be surrounded by several quaternary ammonium groups within a polymer chain or by multiple quaternary ammonium groups between two adjacent polymer chains, thus resulting in ion exchanges between phenolate anions and bromide anions (Br$^-$) via the electrostatic interactions (Fig.S8a). Moreover, the hydrogen of secondary amines (-NH-) of the PDMAPMA chains is probably involved in an intracomplex hydrogen bond with the oxygen of phenol (Fig. S8a). In addition, the residual tertiary amine on the PDMAPMA chains after *N*-alkylation has been demonstrated to act as adsorption site for phenol by weak hydrogen bonding between the hydrogen of phenol and the nitrogen of the tertiary amine (Fig. S8a).[54] To regenerate phenol-loaded microsphere adsorbents with a 0.1 mol·L^{-1} of NaOH solution, it is understandable that he hydroxyl groups can not only the readily eliminate the hydrogen bonding, but also replace the phenolate anions from the polycationic chains via the ion exchange mechanism (Fig. S8b). Therefore, the mixed mechanisms of the ion-exchange via electrostatic interactions and hydrogen bonding are proposed to account for the adsorption and desorption of phenol.

To further validate the postulated mechanisms of the phenol adsorption on the quaternized microspheres, XPS spectrum was characterized on the phenol-loaded microspheres, and is shown in Figure S9 (Supporting Information). The successful adsorption of phenol can be deduced from the noticeable decrease in the relative abundance of Br 3d and N 1s signals (Fig. S9a). The [N]/[C] spectral ratio of about 0.063 is much less than that of the PVBC-g-QPDMAPMA2 microspheres before the phenol adsorption (of about 0.15) (Fig. 6d), and the [O]/[C] spectral ratio reaches as high as 0.33, indicative of the adsorption of henol on the quaternized microsphere surfaces. The significant decrease in the [Br]/[C] ratio is probably caused by the ion exchange of phenolate anions and bromide anionsvia the electrostatic interactions. This result is further ascertained by the appearance of an additional peak component with BE at 286.8 eV in the curve-fitted C 1s core-level spectrum, attributable to the C-O-N species, which is the characteristic bonds of the phenol-loaded microsphere via electrostatic interactions. The persistence of the C-N species in the curve-fitted C 1s core-level spectrum (Fig. S9c) and the >N- species in the curve-fitted N 1s core-level spectrum (Fig. S9d) is consistent with the fact that the secondary amine and the residual tertiary amine of PDMAPMA chains are involved in the adsorption process of phenol.

4. Conclusions

A novel quaternized PDMAPMA-grafted resin with high adsorption capacity of phenolic compounds was developed via surface-initiated ATRP of DMAPMA on the chloromethyl-terminated cross-linked PVBC microspheres, and the subsequent *N*-alkylation reaction to convert pendent tertiary amino groups in the PDMAPMA chains into quaternary ammonium groups. Each functionalization step was ascertained by FTIR XPS and SEM. Batch adsorption studies demonstrated that the adsorption capacity of the so-synthesized microspheres increased linearly with the grafting density of the quaternized PDMAPMA brushes, and that solution pH had little effect on the phenol adsorption in a wide pH range of 3.0-11.0.

The quaternized PDMAPMA-grafted microspheres exhibited ideal sorption behavior for the removal of phenol from aqueous solution in light of adsorption kinetics and sorption capacity. The adsorption equilibrium of phenol on the quaternized microspheres was achieved within 1 h, much fast than that on most of activated carbon and polymeric adsorbents. The maximum adsorption capacity of phenol on the quaternized microspheres from Langmuir-model fitting reached as high as around 2.23 $mmol \cdot g^{-1}$ at pH 6.5, higher than most adsorbents reported. The calculated thermodynamic parameters revealed an exothermic and spontaneous adsorption process of phenol on the quaternized microspheres. Increasing the inorganic salt concentration of $NaNO_3$ and NaCl had a positive effect on the adsorption amount owing to the salting out phenomenon, while organic salt of EDTA showed an adverse effect on the sorption amount of phenol. Furthermore, the quaternized microspheres were proven to have an effective regeneration behavior and quite stable adsorption capacity for repeated applications. Additionally, the postulated adsorption mechanisms were proposed to account for the adsorption process of phenol on the quaternized PDMAPMA-grafted microspheres.

Associated content

Supporting Information. The calibration curve of the phenol aqueous solution and the corresponding UV spectra of the phenol at a wavelength of 504 nm (Figure S1), the optical micrographs and SEM images at different magnifications of the pristine and functionalized PVBC microspheres (Figure S2), the full ATR-FTIR spectra of the surfaces of pristine and PVBC-*g*-PDMAPMA microspheres (Figure S3), the full ATR-FTIR spectra of the surfaces of quaternized PVBC-*g*-QPDMAPMA microspheres (Figure S4), Freundlich-fitted adsorption isotherms at different temperatures (Figure S5), and Temkin-fitted adsorption isotherms at different temperatures (Figure S6), the Van′t Hoff plot for the adsorption of phenol on the quaternized microspheres (Figure S7), the proposed adsorption mechanism of phenol on the quanterinzed PVBC-g-QPDMAPMA microspheres and the regeneration process (Figure S8), and the XPS spectra of the quaternized PDMAPMA-grafted PVBC microspheres after the phenol adsorption (Figure S9).

Acknowledgment

The authors would like to acknowledge the financial assistance of key project of National Natural Science Foundation of China (NO. 21236004).

Notes and references

1. A. Dąbrowski, P. Podkościelny, Z. Hubicki and M. Barczak, *Chemosphere*, 2005, **58**, 1049.
2. Y. Huang, X. Ma, G. Liang and H. Yan, *Chem. Eng. J.*, 2008, **141**, 1.
3. M. Caetano, C. Valderrama, A. Farran and J. L. Cortina, *J. Colloid Interf. Sci.*, 2009, **338**, 402.
4. N. Abdullah, A. Yuzir, T. P. Curtis, A. Yahya and Z. Ujang, *Bioresource Technol.*, 2013, **127**, 181.
5. N. Inchaurrondo, P. Massa, R. Fenoglio, J. Font and P. Haure, *Chem. Eng. J.*, 2012, **198**, 426
6. A. M. Al-Hamdi, M. Sillanpää and J. Dutta, *J. Mater. Sci.* 2014, **49**, 5151.
7. J. Liu, J. Xie, Z. Ren and W. Zhang, *Desalin. Water. Treat.*, 2013, **51**, 3826.
8.A. Bódalo, E. Gómez, A. Hidalgo, M. Gómez, M. Murcia and I. López, *Desalination*, 2009, **245**, 680.
9. L. Damjanovic, V. Rakic, V. Rac, D. Stosic and A. Auroux, *J Hazard Mater*, 2010, **184**, 477.
10. O. Hamdaoui and E. Naffrechoux, *J J Hazard Mater,* 2007, **147**, 381.
11. S. Altenor, B. Carene, E. Emmanuel, J. Lambert, J. J. Ehrhardt and S. Gaspard, *J Hazard Mater,* 2009, **165**, 1029.
12. S. K. Nadavala, K. Swayampakula, V. M. Boddu and K. Abburi, *J Hazard Mater*, 2009, **162**, 482.
13. C. S. Arslan and A. Y. Dursun, *Sep. Sci. Technol.*, 2008, **43**, 3251
14. J. Huang, X. Jin and S. Deng, *Chem. Eng. J.*, 2012, **192**, 192.
15. R. Sharan, G. Singh and S. K. Gupta, *Adsorpt. Sci. Technol.*, 2009, **27**, 267.
16. R. I. Yousef and B. El□Eswed, *Sep. Sci. Technol.* 2007, **42**, 3187.
17. B. Subramanyam and D. Ashutosh, *Int. J. Environ. Res.*, 2011, **6**, 265.
18. M. Ahmaruzzaman and D. Sharma, *J. Colloid Interf. Sci.*, 2005, **287**, 14.
19. A. Gładysz-Płaska, M. Majdan, S. Pikus and D. Sternik, *Chem. Eng. J.*, 2012, **179**, 140.
20. S. Rio, C. Faur-Brasquet, L. Le Coq and P. Le Cloirec, *Environ. Sci. Technol.*, 2005, **39**, 4249.
21. A. Namane and A. Hellal, *J. Hazard Mater*, 2006, **137**, 618.
22. M. L. Soto, A. Moure, H. Domínguez and J. C. Parajó, *J. Food Eng.* 2011, **105**, 1.
23. G. Pigatto, A. Lodi, E. Finocchio, M. S. Palma and A. Converti, *Chem. Eng. Process.* 2013, **70**, 131.
24. S. Sagbas, C. Kantar and N. Sahiner, *Water Air Soil Poll.* 2014, **225**, 1.
25. R. Aravindhan, J. R. Rao and B. U. Nair, *J. Environ. Manage*, 2009, **90**, 1877.
26. İ. Abay, A. Denizli, E. Bişkin and B. Salih, *Chemosphere*, 2005, **61**, 1263.
27. A. A. H. Al-Muhtaseb, K. A. Ibrahim, A. B. Albadarin, O. Ali-Khashman, G. M. Walker and M. N. Ahmad, *Chem. Eng. J.*, 2011, **168**, 691..
28. E. Vismara, L. Melone, G. Gastaldi, C. Cosentino and G. Torri, *J. Hazard Mater.* 2009, **170**, 798.
29. Z. W. Ming, C. J. Long, P. B. Cai, Z. Q. Xing and B. Zhang, *J. Hazard Mater*. 2006, **128**, 123.
30. D. Jermakowicz-Bartkowiak, B. Kolarz and A. Serwin, *React. Funct. Polym.* 2005, **65**, 135.
31. S. Samatya, N. Kabay and A. Tuncel, *J. Appl. Polym. Sci.* 2012, **126**, 1475.
32. S. Margel, E. Nov and I. Fisher, *J. Polym. Sci. Pol. Chem.* 1991, **29**, 347.
33. L. Gao, C.-Y. V. Li, K. Y. Chan and Z.-N. Chen, *J. Am. Chem. Soc.* 2014, **136,** 7209.
34. R. Sellin and S. D. Alexandratos, *Ind. Eng. Chem. Res.* 2013, **52**, 11792.
35. O. E. Fayemi, A. S. Ogunlaja, P. F. Kempgens, E. Antunes, N. Torto, T. Nyokong and Z. R. Tshentu, *Miner. Eng.*, 2013, **53**, 256.
36. D. Kaner, A. Saraç and B. F. Şenkal, *Environ. Geochem. Hlth.*, 2010, **32**, 321.
37. G. G. Huang and J. Yang, *Anal. Chem.* 2003, **75**, 2262.

38. H. C. Lin, Y. H. Chou and J. Yang, *Anal. Chim. Acta*, 2008, **611**, 89.
39. F. Bildik, G. T. Turan, G. Barım and B. F. Senkal, *Sep. Sci. Technol.* 2014, 49, 1700.
40. E.Nicol, A. Moussa, J.-L. Habib-Jiwan and A. M. Jonas, *J. Photoch. Photobio. A*, 2004, **167**, 31.
41. D. J. Siegwart, J. K. Oh and K. Matyjaszewski, *Prog. Polym. Sci.*, 2012, **37**, 18.
42. Z. Cheng, X. Zhu, Z. Shi, K. Neoh and E. Kang, *Ind. Eng. Chem. Res.* 2005, **44**, 7098.
43. X. Zhang, G. Li, H. Zhang, X. Wang, J. Qu, P. Liu and Y. Wang, *Soft Matter*, 2013, **9**, 6159.
44. A. A. H. Al-Muhtaseb, K. A. Ibrahim, A. B. Albadarin, O. Ali-khashman, G. M. Walker and M. N. M. Ahmad, *Chem. Eng. J.*, 2011, **168**, 691.
45. E. Yavuz, G. Bayramoğlu, B. F. Şenkal and M. Y. Arıca, *J. Chromatogr. B*, 2009, **877**, 1479.
46. Z. Cheng, L. Zhang, X. Zhu, E. Kang and K. Neoh, *J. Polym. Sci. Pol. Chem.* 2008, **46**, 2119.
47. T. Saito, S. Brown, S. Chatterjee, J. Kim, C. Tsouris, R. T. Mayes, L.-J. Kuo, G. Gill, Y. Oyola and C. J. Janke, *J. Mater. Chem. A*, 2014, **2**, 14674.
48. J. Ye, L. P. Sun and S. P. Gao, *Adv. Mater. Res*, 2013, **704**, 270.
49. S. Deng, Y. Zheng, F. Xu, B. Wang, J. Huang and G. Yu, *Chem. Eng. J.* 2012, **193**, 154.
50. S. J. Yuan, G. M. Xiong, X. Y. Wang, S. Zhang and C. Choong, *J. Mater. Chem.* 2012, **22**, 13039.
51. R. Barbey, L. Lavanant, D. Paripovic, N. Schüwer, C. Sugnaux, S. Tugulu and H.-A. Klok, *Chem. Rev.*, 2009, **109**, 5437.
52. S. J. Yuan and S. O. Pehkonen, *Colloid Surf. B* 2007, **59**, 87.
53. E. W. Rice and A. P. H. Association, *Standard methods for the examination of water and wastewater*, American Public Health Association Washington, DC, 2012.
54. M. Jiang, J. Wang, L. Li, K. Pan and B. Cao, *RSC Adv.* 2013, **3**, 20625.
55. İ. Y. İpek, N. Kabay, M. Yüksel, D. Yapıcı and Ü. Yüksel, *Desalination*, 2012, **306**, 24.
56. G. Bayramoglu, E. Yavuz, B. F. Senkal and M. Y. Arica, *Colloid Surface A* 2009, **345**, 127.
57. S. D. Alexandratos and X. Zhu, *Macromolecules*, 2003, **36**, 3436.
58. J. F. Moulder, W. F. Stickle, P. E. Sobol and K. D. Bomben, *Handbook of X-ray photoelectron spectroscopy*, Perkin Elmer Eden Prairie, MN, 1992.
59. Z. Y. Yang, S. J. Yuan, B. Liang, Y. Liu, C. Choong, S. O. Pehkoen, *Macromol. Biosci.* 2014, **14,** 1299.
60. Y. Liu, L. Wang and C. Pan, *Macromolecules*, 1999, **32**, 8301.
61. W. J. Barreto, S. Ponzoni and P. Sassi, *Spectrochim. Acta A* 1998, **55**, 65.
62. X. Lv, Y. Li and M. Yang, *Polym. Advan. Technol.* 2009, **20**, 509.
63. D. Roy, J. S. Knapp, J. T. Guthrie and S. Perrier, *Biomacromolecules*, 2007, **9**, 91.
64. S. B. Deng, Y. Q. Zheng, F. J. Xu, B. Wang, J. Huang and G. Yu, *Chem. Eng. J.* 2012, **193-194**, 154.
65. Q. S. Liu, T. Zheng, P. Wang, J. P. Jiang and N. Li, *Chem. Eng. J.*, 2010, **157**, 348.
66. A. T. Mohd Din, B. Hameed and A. L. Ahmad, *J. Hazard. Mater.* 2009, **161**, 1522.
67. J. Fan, W. Yang and A. Li, *React. Funct. Polym.* 2011, **71**, 994.
68. L. Zhu, Y. Deng, J. Zhang and J. Chen, *J. Colloid Interf. Sci.* 2011, **364**, 462.
69. P. J. Silva, *J. Org. Chem.* 2008, **74**, 914.
70. U. Thawornchaisit and K. Pakulanon, *Bioresource Technol.*, 2007, **98**, 140.
71. L. Q. Huang, S. J. Yuan, L. Lv, G. Q.Tan, B. Liang and S. O. Pehkonen, *J. Colloid Interf. Sci.* 2013, **405**, 171.
72. G. Yang, L. Tang, G. Zeng, Y. Cai, J. Tang, Y. Pang, Y. Zhou, Y. Liu, J. Wang and S. Zhang, *Chem. Eng. J.*, 2015, **259**, 854.
73. Y. Chen, M. He, C. Wang and Y. Wei, *J. Materi. Chem. A*, 2014, **2**, 10444.
74. G. Barassi, A. Valdés, C. Araneda, C. Basualto, J. Sapag, C. Tapia and F. Valenzuela, *J. Hazard. Mater.* 2009, **172**, 262.
76. J. C. Lazo-Cannata, A. Nieto-Márquez, A. Jacoby, A. L. Paredes-Doig, A. Romero, M. R. Sun-Kou and J. L. Valverde, *Sep. Purif. Technol.* 2011, **80**, 217.
76. A. Soto, A. Arce, M. K Khoshkbarchi and J. H. Vera, *Biophys. Chemistry*, 1998, **73**, 77.
77. J. C. Lazo-Cannata, A. Nieto-Márquez, A. Jacoby, A. L. Paredes-Doig, A. Romero, M. R. Sun-Kou and J. L. Valverde, *Sep. Purif. Technol.*, 2011, **80**, 217.
78. I. Tan, A. L. Ahmad and B. Hameed, *J. Hazard. Mater.* 2008, **154**, 337.

TOC Graphic

Title: Purification of phenol-contaminated water by adsorption with quaternized poly(dimethylaminopropyl methacrylamide)-grafted PVBC microspheres

Authors: Juntao Gu, Shaojun Yuan,[a,*] Yu Zheng, Wei Jiang, Bin Liang, Simo O Pehkonen

The cross-linked PVBC microspheres were tethered with quaternized PDMAPMA brushes via surface-initiated ATRP as effective anionic sorbents for phenol removal